AIDDATA
A Research Lab at William & Mary

WORKING PAPER 49

May 2018

Geostatistical Tools to Map the Interaction between Development Aid and Indices of Need

Claudio Bosco
WorldPop, Department of Geography and Environment,
University of Southampton, UK
Flowminder Foundation, Stockholm, Sweden

Natalia Tejedor-Garavito
WorldPop, Department of Geography and Environment,
University of Southampton, UK
Flowminder Foundation, Stockholm, Sweden

Daniele de Rigo
Maieutike Research Initiative, Milano, Italy

Andrew J. Tatem
WorldPop, Department of Geography and Environment,
University of Southampton, UK
Flowminder Foundation, Stockholm, Sweden

Carla Pezzulo
WorldPop, Department of Geography and Environment,
University of Southampton, UK
Flowminder Foundation, Stockholm, Sweden

Richard Wood
Flowminder Foundation, Stockholm, Sweden

Heather Chamberlain
WorldPop, Department of Geography and Environment,
University of Southampton, UK
Flowminder Foundation, Stockholm, Sweden

Tom Bird
WorldPop, Department of Geography and Environment,
University of Southampton, UK
Flowminder Foundation, Stockholm, Sweden

Abstract

In order to meet and assess progress towards global sustainable development goals (SDGs), an improved understanding of geographic variation in population wellbeing indicators such as health status, wealth and access to resources is crucial, as the equitable and efficient allocation of international aid relies on knowing where funds are needed most. Unfortunately, in many low-income countries, detailed, reliable and timely information on the spatial distribution and characteristics of intended aid recipients are rarely available. Furthermore, lack of information on the past distribution of aid relative to need also hinders assessments of the impacts of aid. High-resolution data on key social and health indicators, as well as how aid distribution relates to these indicators are therefore fundamental for targeting limited resources and building on past efforts.

In this study, we show how modern statistical approaches combined with a new geographic database of aid distribution can be used to map the distribution of indicators with a level of detail that can support geographically stratified decision-making. Based on geo-located survey data from Demographic and Health Surveys (DHS) in Nigeria (2008 - 2013) and Nepal (2006 - 2011), Bayesian geostatistical models and machine learning approaches were used in combination with a suite of spatial data layers to create high-resolution predictive maps for (i) the rates of stunting in children under the age of five and (ii) the household wealth index. An ensemble model was also exploited for aggregating different modelling results to improve the modelling prediction capacity in Nigeria (for stunting 2008). By combining these maps with information on the disbursement of aid for increasing food security and alleviating poverty (AidData database - http://aiddata.org/), we quantified both the reported spatial distribution of aid relative to stunting and poverty, as well as how changes in these indices over time related to aid disbursement. While many cases of aid disbursement lacked detailed spatial information, the results here demonstrate the potential of this approach and highlight the value of spatially disaggregated data on the distribution of aid.

Author Information

Claudio Bosco
WorldPop, Department of Geography and Environment, University of Southampton, UK
Flowminder Foundation, Stockholm, Sweden

Natalia Tejedor-Garavito
WorldPop, Department of Geography and Environment, University of Southampton, UK
Flowminder Foundation, Stockholm, Sweden

Daniele de Rigo
Maieutike Research Initiative, Milano, Italy

Andrew J. Tatem
WorldPop, Department of Geography and Environment, University of Southampton, UK
Flowminder Foundation, Stockholm, Sweden

Carla Pezzulo
WorldPop, Department of Geography and Environment, University of Southampton, UK
Flowminder Foundation, Stockholm, Sweden

Richard Wood
Flowminder Foundation, Stockholm, Sweden

Heather Chamberlain
WorldPop, Department of Geography and Environment, University of Southampton, UK
Flowminder Foundation, Stockholm, Sweden

Tom Bird
WorldPop, Department of Geography and Environment, University of Southampton, UK
Flowminder Foundation, Stockholm, Sweden

Acknowledgments

This article benefited from helpful conversations with Jessica Cohen, Günther Fink, Kristen Himelein, Jon Kastelic, John Marshall, Horacio Larreguy, Dan Rogger, and seminar audiences at the Harvard School of Public Health, the Working Group on African Political Economy (WGAPE), APSA, ASA, and the World Bank

Contents

List of Acronyms and Abbreviations

AIMS	Aid Information Management System - are information and communication technology applications that enable donors and recipient governments to open and share aid data
AMORE	A MORE flexible neural network - is a Neural Network package born to release a robust neural network algorithm to the R users
AMP	Aid Management Platform
ANN	Artificial Neural Network
BGS	Bayesian Geostatistical
CEDA	Centre for Environmental Data Analysis
CIESIN	Centre for International Earth Science Information Network
DAD	Development Assistance Database - is an Aid Information Management System developed by Synergy International Systems, for tracking development aid and managing official development assistance
DEM	Digital Elevation Model
DHS	Demographic and Health Surveys – the DHS Program assists developing countries worldwide in the collection and use of data to monitor and evaluate population, health, and nutrition programs.
D-TM	Data-Transformation Model - a D-TM is a conceptual unit which transforms a set of input data and model parameters into a corresponding set of output data.
EA	Enumeration Area – is the operational geographic units for the collection of census data
ESA	European Space Agency
EVI	Enhanced Vegetation Index – is an 'optimized' vegetation index designed to enhance the vegetation signal with improved sensitivity in high biomass regions and improved vegetation
GeoSemAP	Geospatial Semantic Array Programming - geospatial application of the SemAP paradigm, where the conceptual units (D-TMs) of the modelling workflow are a composition of geospatial transformations and array-based D-TMs.
GHSL	Global Human Settlements Layer – is a dataset containing new global spatial information, evidence-based analytics and knowledge describing the human presence on the planet
GNI	Gross National Income
GRUMP	Global Rural Urban Mapping Project
HOT	Humanitarian OpenStreetMap Team
INLA	Integrated Nested Laplace Approximations – is a package (in R) that exploit the approach of Integrated Nested Laplace Approximations to do approximate Bayesian inference for latent Gaussian models.

IWI	International Wealth Index - is similar to the widely used WI included in the DHS, but adds the property of comparability across place and time.
LSMS	Living Standards Measurements Study - is a household survey program focused on generating high-quality data, improving survey methods, and building capacity
MAE	Mean Absolute Error
MICS	Multiple Indicator Cluster Survey – is one of the largest household survey program (developed by UNICEF) on children's and women's well-being
OSM	Open Street Map – is a project that creates and distributes free geographic data for the world.
PCA	Principal Component Analysis
PPS	Probability Proportion to Size - is a method of sampling where a size measure is available for each population unit before sampling and the probability to select a unit is proportional to its size.
PSU	Primary Sampling Unit - refers to sampling units that are selected in the first (primary) stage of a multi-stage sample ultimately aimed at selecting individual elements
RMSE	Root Mean Square Error
SemAP	Semantic Array Programming - a computational modelling approach to compactly process arrays of data preserving the consistency of their underpinning semantics. SemAP is based on the modularisation of the modelling workflow into conceptual units (modules) of data-transformation (see D-TM), and on the systematic use of array-based semantic constraints.
SIEVE	Selective Improvement Evolutionary Variance Extinction - Training architecture for nonlinear computational models, such as artificial neural networks.
SPDE	Stochastic Partial Differential Equations
SRTM	Shuttle Radar Topography Mission - is an international research effort that obtained digital elevation models on a near-global scale from 56° S to 60° N
WDPA	World Database on Protected Areas
WHO	World Health Organization
WI	Wealth Index - is a measure to indicate inequalities in household characteristics, in the use of health and other services, and in health outcomes

1. Background and Objectives

Equitable and efficient allocation of international aid relies on knowing where resources are needed most. For instance, aid for poverty alleviation or financial access improvement requires knowledge of where the poor are (Steele et al, 2017), aid for maternal and newborn health requires information on local births, pregnancy rates (Tatem et al., 2014), and infant mortality rates (Pezzulo et al., 2016; Golding et al., 2017). Unfortunately, detailed, reliable and timely information on the spatial distribution and characteristics of intended aid recipients in many low income countries are rarely available, impacting the ability of aid agencies to effectively and equitably distribute resources to those most in need. A similar paucity of spatially-explicit information on where aid money has been spent hinders assessments of the impacts of aid projects. In the past, the information about how aid moneys were distributed tended to be kept internally within aid agencies or governments (Schulz, 2009). Data on the spatial distribution of funds were difficult to record or track and sharing of detailed information between agencies was uncommon, leading to inefficiencies and corruption (Christensen *et al,* 2010, Drabek and Payne, 2002). Tracking, monitoring and determining the impacts of interventions presents significant logistical challenges, particularly where multiple overlapping initiatives take place. As a consequence of poorly defined spatial data on both those in need and how money has been spent, aid agencies and governments globally are focussing on the importance of spatial data for understanding how to allocate aid resources.

Increasingly, information on socio-economic wellbeing are becoming more specific and spatially disaggregated. Indices of need can be derived from demographic measures obtained from individual-based surveys, the majority of which now record anonymized spatial data on the locations of surveys. Indices of poverty rely on knowing the proportion of individuals in the population that exceed a certain income, consumption or asset threshold. In many cases, census data may provide the relevant information, and can be used to accurately depict the status of a population, sometimes at the level of enumeration areas or cities. However, enumeration area-level census data can often be outdated or unreliable, or simply hard to obtain, particularly when matching to GIS-format boundary files is required, and particularly in low-income countries where accurate depictions of need are most urgently needed (Tatem, 2014).

An alternative approach to the comprehensive measurement that census data provide is to use random subsampling to obtain a representative sample of the population. Contemporary geolocated household survey data from the Demographic and Health Surveys (DHS) (http://dhsprogram.com), Living Standards Measurements Study (LSMS) (Grosh and Glewwe, 1995; World Bank, 2016), and Multiple Indicator Cluster Survey (MICS) (http://mics.unicef.org), etc.), for example, have a growing presence in the social sciences and have been used extensively to provide broad-scale estimates of factors such child mortality, nutrition and poverty. Such surveys can be used to enrich census-based data or, where census data are outdated, unavailable or unreliable, infer values at unobserved locations using predictive modelling. However, typically such surveys are only considered representative at regional levels and as such tend to be aggregated over areas that are too large to provide detailed spatial information. Furthermore, such

representative surveys rarely cover all areas of interest, often leaving large areas unsampled due to logistical, security or other reasons (Schulz, 2009).

To make up for the gaps and the low resolution of sampled survey data, modelling approaches can be used to infer values for population welfare indicators where they have not been recorded. Spatial demographic modelling approaches take advantage of the fact that many human population characteristics are correlated to environmental or sociological factors (Cliff and Ord, 1975). While the causative factors of population wellbeing indicators may be due to multiple political, environmental and cultural factors, the consequences of poverty often manifest in physical and geographic terms in ways that are measurable using an array of spatial data features. For example, poverty measure at population levels have been linked to the intensity of nightlights visible from space (Jean *et al*, 2016), mobile phone data (Blumenstock *et* al, 2015; Steele *et* al, 2017) and road infrastructure (Gibson and Roxelle, 2003). Similarly, proximity to roads and access to hospital and food resources in urban settings may correlate with indices of nutrition (Okwi *et al,* 2007; Minot *et al,* 2006). Work in Africa has shown vegetation cover and indices of greenness, to be associated with the proportion of children under 5 (Alegana *et al,* 2015). With the increasing availability of high-resolution global satellite data, many such correlative spatial variables are available nowadays as gridded spatial datasets (Lloyd *et al,* 2017). Harnessing the correlative power of these covariates in spatially-explicit statistical models is an increasingly important means of increasing the utility of survey datasets by allowing for disaggregated insights at finer spatial scales and inference in locations where data were never recorded (e.g. Bosco et al., 2017a, 2017b; Alegana et al., 2015; Sedda et al., 2015, Golding et al., 2017). It is here important to remark how correlation of particular population wellbeing indicators with selected environmental or sociological factors does not automatically imply them to be causative factors. In other words, while modelling wellbeing indicators with the help of environmental or sociological factors is unable to explicitly reconstruct underpinning causative relationships, it nevertheless can improve our ability to reconstruct *higher resolution spatial patterns* - otherwise unknown – of wellbeing indicators.

Here we use Bayesian geostatistical (BGS) and machine learning methods based on geolocated surveys and census data in combination with gridded spatial covariate layers to construct fine spatial resolution maps of stunting and wealth index in Nepal and Nigeria. This approach also allows us to estimate associated metrics of model uncertainty, highlighting where predictions made are more confident versus areas where there is high uncertainty due to either a lack of surveys, conflicting data from surveys or poor explanatory power from the selected covariate layers. Using these modelling architectures, we then explore the interaction of aid with both poverty and stunting at sub-national scales where such data were available. Finally, we compare changes in the indices of need against the level of aid given in each area in order to determine whether observable changes in the associate indices were apparent.

2. The Context

Nigeria and Nepal are characterised by having a low or medium-low human development index (UNDP, 2016). They are ranked respectively 144 (Nepal) and 152 (Nigeria) out of 188 countries

worldwide. Nigeria, in common with many other countries in sub-Saharan Africa, is characterized by high population growth, low or medium-low gross national income (GNI) per capita and a high poverty rate (World Bank, 2016). The mean annual population growth rate is 2.6% and GNI per capita, calculated using the Atlas method, is $2450, with almost half of the population below the national poverty line (World Bank, 2016). Around 37% of children under age five in Nigeria are stunted with a slight difference between males and females (39% versus 35%, NPC, 2014). Nepal is characterized by a mean annual population growth rate of 1.1% with a GNI per capita calculated using the Atlas method of $730. Available data (MOHP, 2012) showed that 41 percent of children under age 5 are stunted, and 16 percent are severely stunted. The level of stunting is similar in male (41%) and female (40%) children. With respect to the wealth index, there is a high degree of spatial variability in the distribution of wealth, with the overwhelming majority of urban residents (62 percent) being from the richest quintile, while a much lower proportion of rural residents (14 percent) fall in the same category. Less than 1 percent of the population in the mountain zone (0.5 percent) is in the highest wealth quintile.

3. Material and Methods

3.1 Datasets

In the present study, we exploit the publically available Demographic Household Survey (DHS) data for Nepal and Nigeria (NPC and ICF, 2009, 2014; MOHP et al., 2007, 2012), focussing on indicators of malnutrition and household wealth. These population-welfare data are compared to data on the distribution of aid moneys in these countries derived from the AidData database established by USAID (www.AidData.org).

3.1.1 DHS indicators and DHS based indicators

The Demographic Household Survey (DHS) program regularly conducts household surveys in many low-income countries around the world. These surveys are considered to be a reliable and efficient way for collecting population welfare information that are representative at the national level. With the aim of providing nationally-representative data with a more rapid frequency than is possible with a standard census, the DHS program adopts a globally-recognised sampling design, usually using a two (or three) stage cluster sampling procedure (ICF International, 2012). Primary sampling units (PSUs) are usually defined as households within clusters of between 10 and 40 households within pre-existing census enumeration areas (EAs). Following standard sampling procedures, a stratified sample of EAs is usually selected with probability proportional to size (PPS) (ICF International, 2012), where the country census bureau usually provides the definition of the sampling weights and boundaries of EAs. Urban and rural areas are also differentiated, and the definitions of EAs can differ between these classes. For example, an EA in an urban area might be defined as part or all of a city block, whereas rural EAs might include one or more villages, with the typical number of households falling between 100 and 300. In the second stage of sampling a fixed (or variable) number of between 10 and 40 households within each EA is selected and every eligible adult in the selected households is interviewed (ICF International, 2012) (Gething et al., 2015). In more recent surveys, the geographic coordinate of the estimated centre of each cluster is recorded and given a unique cluster identifier. In order to protect the anonymity of survey

respondents but to retain some level of geographic representivity, the cluster locations are anonymized through a spatial displacement process wherein each cluster centroid is displaced a random distance (up to 2 km in urban settings and 5 km in rural) in a random direction. Furthermore, around 1% of the rural clusters was displaced up to 10 km (Macro International Inc., 1996; Burgert et al. 2013). We used the publicly available DHS survey data and related cluster GPS coordinates for Nigeria (2008 and 2013) and Nepal (2006 and 2011) were obtained. The following sections describe the indicators we mapped. Specifically, we chose indicators (Stunting and wealth index) which are known to have strong spatial dimensions (Bosco et al., 2017a; Steele et al., 2017).

3.2 Stunting in Children

We first looked at stunting in children as this indicator can be linked to environmental factors leading to low caloric intake. Specifically, factors such as poverty and agriculture yields have been linked to stunting in past work (Gething *et al*., 2015). Child anthropometric measures used in this work were calculated following DHS instructions and country specific final report indications (ICF International, 2012). The measure of stunting we used here comes from the height-for-age Z-scores. Children whose height-for-age Z-score is more than two standard deviations (-2 SD) below the median of the WHO (WHO, 2006) reference population are considered short for their age (stunted) and chronically malnourished. The geolocated cluster-level proportions of stunted children were used in our analyses.

3.3 Wealth Index

The wealth index (WI) used in this survey is a measure that has been used in many DHS and other country level surveys to indicate inequalities in household characteristics, in the use of health and other services, and in health outcomes (Rutstein et al., 2000). The index was constructed using household asset data via a principal components analysis (PCA). In its current form, which takes better account of urban-rural differences in scores and indicators of wealth, the wealth index is created in three steps. This three-step procedure permits greater adaptability of the wealth index in both urban and rural areas (Rutstein, 2008; Rutsein and Kiersten, 2004) (https://www.dhsprogram.com/topics/wealth-index/index.cfm).

3.4 International Wealth Index

While the DHS-derived wealth index is intended to be relatively accurate within the context of individual countries and years, its comparability over time has been questioned. To allow comparability across years, we explored the use of the International Wealth Index (IWI) for assessing wealth in Nigeria and Nepal. The IWI is an asset-based index for household's material well-being and it gives an indication of long-term economic status. While similar in construction to wealth indices collected by Demographic and Health Surveys (DHS) and the Multiple Indicator Clusters Surveys (MICS) collected by UNICEF, the methods developed by Smits and Stendijk (2015) to construct the IWI allows for comparability over time and space. We derived the IWI using the DHS household data for all the needed years and countries.

3.4.1. The AidData Database

Information on the distribution of aid money for alleviation of poverty (table 1) and malnutrition in Nepal (table 1) and in Nigeria (table 2) came from the AidData database. AidData has an open data portal where the locations of investments at the sub-national level are available. For this research

we used the 1.3.1 version of the Level 1 product for Nigeria and 1.3 version for Nepal. All geocoded projects for Nigeria came from the Development Assistance Database (DAD) Aid Information Management System (AIMS) (AidData, 2016a) and for Nepal from the Aid Management Platform (AMP) Aid Information Management System (AIMS) (AidData, 2016b). These data sets consist of geographical locations of the different investments identified in Nigeria and Nepal, with (in most cases) their financial commitment and disbursement. The precision of the investment locations vary depending on the information available, ranging from data on the exact location of disbursement through to records that only indicate that the funds were allocated somewhere within the country as a whole, where in the latter case it is likely that the funding went to a government ministry or financial institution. In this project, the data were filtered to select those projects with locations and disbursement and commitment that related to stunting and poverty and covered the period between 2000 and 2020. For stunting, projects were included if they were related to women/maternal/newborn health, women's inclusion in society, education, agricultural projects at the local scale, water supply and sanitation. For poverty most of the projects related to health, food security, nutrition, banking and financial services, energy generation and transport, among others.

The most promising results, in terms of relating indices of poverty to aid spending were obtained in Nepal, where 63% of money related to the wealth index are geocoded. Based on conversations with government officials and aid organisations in-country, we decided to re-allocate the 37% of non-geo-located funds following the real distribution of the geolocated disbursement.

Table 1: Summary of database for all data available and those projects related to poverty and stunting in Nepal

Data	**All projects**	**Related to stunting**	**Related to poverty**
Start year (min)	1997	1999	1997
End year (max)	2014	2013	2013
Donors	110	67	78
Total Projects	873	397	604
Geocoded Projects	373	227	322
Locations	20815	18185	19718
Total Disbursements	$4,287,879,756	$1,939,259,874	$3,978,396,085
Total Commitments	$8,923,101,534	$3,661,993,814.	$7,021,467,010
Geocoded Disbursements	$2,572,575,662	$1,695,047,995	$2,503,157,637
Geocoded Commitments	$4,758,802,627	$3,355,819,271	$4,513,527,205

Table 2: Summary of database for all data available and those projects related to stunting in Nigeria

Data	All projects	Related to stunting
Start year (min)	1988	2002
End year (max)	2020	2017
Donors	28	12
Total Projects	621	271*
Geocoded Projects	595	103
Locations	1843	483
Total Disbursements	$6,255,493,636	$5,575,541,874
Total Commitments	$2,144,374,320	$1,538,242,430
Geocoded Disbursements	$6,093,125,384	$2,833,812,856
Geocoded Commitments	$2,116,331,293	$717,178,638

*263 with disbursement or commitment

3.5 Geospatial Covariate Layers

Given that the aim of the analyses was to compare estimates of population welfare indicators at high spatial resolution against spatial distribution of aid funding, we used geospatial modelling procedures to create high resolution maps for the indicators in question. To do so, we exploited correlative relationships between the indicators and covariates layer, in combination with models also accounting for spatial autocorrelation between sample points. In order to conduct this kind of geospatial modelling, we selected a number of covariates from existing publicly available datasets and libraries, based on factors that have previously been shown to correlate with stunting and wealth index in different settings (Bosco et al., 2017a, 2017b). Several physical (topography, potential evapotranspiration, land cover, etc.) and some social (e.g. population density) covariate grids derived from public available datasets were selected and tested as possible explanatory covariates across the analysed DHS indicators. All spatial datasets were processed to have a spatial resolution of 0.0083 decimal degrees (approximately 1km at the Equator) Tables 3 and 4 provide the sources for these data as well as naming conventions used for Nepal and Nigeria. Descriptions of these data types are provided below.

Table 3: Details of geospatial covariates assembled for mapping malnutrition and poverty in Nepal

Dataset name	Continuous or categorical	Data source	Year
Accessibility	Continuous	European Commission Joint Research Centre	2000
Population count	Continuous	WorldPop	2010
Potential Evapotranspiration	Continuous	CEDA	2001-2012
GHSL	Continuous	Global Human Settlement Layer	2000, 2014

Nightlight	Continuous	NOAA	2007, 2010
Elevation	Continuous	CGIAR-CSI (SRTM)	2003
MODIS EVI	Continuous	MODIS MOD13A1 [Enhanced vegetation index]	2010-2014
Distance to roads	Continuous	Input data from OSM (http://extract.bbbike.org/)	2015
Distance to waterways	Continuous	Input data from OSM (http://extract.bbbike.org/)	2014
Percentage of Urban Areas	Continuous	CIESIN - Global Rural Urban Mapping Project	2000
Protected Areas	Categorical	WDPA (http://www.protectedplanet.net/)	2012
Landcover	Categorical	ESA	2005, 2010
Precipitation	Continuous	CEDA	2001-2012
Temperature	Continuous	CEDA	2001-2012
Latitude	Continuous	Input data from Worldpop	2015
Longitude	Continuous	Input data from Worldpop	2015

Table 4 - Details of geospatial covariates assembled for mapping malnutrition in Nigeria

Dataset name	**Continuous or categorical**	**Data source**	**Year**
Accessibility	Continuous	European Commission Joint Research Centre	2000
Nightlight	Continuous	NOAA	2010, 2013
Temperature	Continuous	CEDA	2001-2012
MODIS EVI	Continuous	MODIS MOD13A1 [Enhanced vegetation index]	2001-2005
Population count	Continuous	WorldPop Project	2010
Distance to roads	Continuous	Input data from OSM (http://extract.bbbike.org/)	2014
Elevation	Continuous	USGS	2001
Potential evapotranspiration	Continuous	CEDA	2001-2012
Percentage of urban areas	Continuous	Input data from "WorldPop Project"	2010
GHSL	Continuous	Global Human Settlement Layer	2000, 2014

Distance to conflicts	Continuous	Input data from ACLED	2010-2013
e-RUSLE LS factor	Continuous	WorldPop	2017
Precipitation	Continuous	CEDA	2001-2012
Protected areas	Categorical	WDPA (http://protectedplanet.net/)	2012
Distance to rivers	Continuous	Input data from VMAP0	Multiple years
Landcover	Categorical	ESA	2005, 2010

3.5.1 Accessibility

The EU Joint Research Center created a gridded surface estimating accessibility, measured in likely travel times, to cities having a population over 50,000 inhabitants (Nelson, 2008). Accessibility was defined to include both land-based (road/off-road) and water-based (navigable river, lake and ocean) travel. This measure provides context on a degree of urbanicity and connectivity for each 1 x 1 km grid pixel, and takes into account both the road distance and type of road such that places near major roads are considered to be better connected (and have lower travel times) than areas with minor roads. More details of this geospatial layer can be found at http://forobs.jrc.ec.europa.eu/products/gam.

3.5.2 Elevation

A digital elevation model (DEM) derived from the NASA 2000 Shuttle Radar Topography Mission (SRTM) was obtained (Jarvis et al., 2008). The CGIAR-CSI SRTM v4.1 provides continuous elevation data coverage, through the use of a void-filling algorithm. This is especially relevant in mountainous regions due to the original SRTM DEM having large no data extents. The SRTM v4.1 DEM has a spatial resolution of 3 arc seconds (approximately 90m) resampled to approximately 1km. The data were resampled using nearest neighbour resampling. (Consultative Group for International Agricultural Research Consortium for Spatial Information http://srtm.csi.cgiar.org/).

3.5.3 Nightlights

Composite nightlight imagery for 2007 and 2011 in Nepal and, 2010 and 2013 in Nigeria were obtained (http://ngdc.noaa.gov/eog/) (NOAA, 2014). This data was available as DMSP-OLS Nighttime Lights v4 Time Series. Annual night light intensity data was extracted as: Average Visible, Stable Lights, and Cloud Free Coverages, at ~ 1 km spatial resolution.

3.5.4 MODIS mean Enhanced Vegetation Index (EVI)

MODIS 16-day L3 Global EVI (MOD13Q1) composite data are collected by the MODIS (Moderate Resolution Imaging Spectroradiometer) sensor aboard NASA's TERRA satellite. MODIS EVI products are computed from atmospherically corrected bi-directional surface reflectances that have been masked for water, clouds, heavy aerosols, and cloud shadows (LP DAAC, 2001). Vegetation indices are an indicator of green vegetation growth and density. MOD13Q1 data have a spatial resolution of 250m. A seamless raster covering Nepal and Nigeria was created through geo-referenced mosaicking in different time intervals.

Source: USGS LP DAAC (Land Processes Distributed Active Archive Center) - MOD13Q1 accessed and projected using the MODIS Reprojection Tool Web Interface (MRTWeb - http://mrtweb.cr.usgs.gov/ImgViewer/Java2ImgViewer.php)

3.5.5 e-RUSLE LS factor

The LS factor of the e-RUSLE model (Bosco et al., 2015) considers the flows convergence and quantifies the combined effect of slope length and slope steepness on soil erosion. It is the result of the combination of the slope (S) and length (L) factors of the e-RUSLE model. It has been created starting from the SRTM.

3.5.6 Protected Areas

Protected areas were obtained from the World Database on Protected Areas (WDPA), available through (IUCN & UNEP–WCMC, 2012). Protected areas are represented as vector polygons, which were converted to a binary raster.

3.5.7 Distance to Rivers

The "Distance to waterways" covariate was calculated using the most recent Open Street Map river network dataset (https://www.openstreetmap.org/) available at the time of analysis, with distances calculated using ArcGIS Euclidean Distance tool.

3.5.8 Distance to Roads

The "Distance to roads" covariate was calculated using the Open Street Map (OSM) road network dataset (https://www.openstreetmap.org/). OSM data coverage for Nepal increased rapidly following the April 2015 earthquake due to requests for mapping needs released via the Humanitarian OpenStreetMap Team (HOT). In particular, many of the mapping tasks involved digitisation of roads and transport infrastructure. However the increase in coverage was concentrated in earthquake-affected areas, leading to spatial heterogeneity in OSM data coverage across Nepal. To account for this spatial bias, only roads classified as 'primary', 'primary_link', 'residential', 'secondary', 'secondary_link', 'tertiary', 'trunk', 'trunk_link' or 'road' were included. Distances were calculated using ArcGIS Euclidean Distance tool.

3.5.9 Land Cover

Landcover data was available as maps at 300 m spatial resolution corresponding to the different epochs 2000 (from 1998 to 2002), 2005 (from 2003 to 2007), 2010 (from 2008 to 2012), version (v.1.6.1), obtained from the European Space Agency (ESA) (ESA, 2014).

3.5.10 Climatic Variables

The annual mean of monthly temperature (°C), precipitation (mm), and potential evapotranspiration for every year from 2001-2012, at ~50km spatial resolution, was extracted from the Centre for Environmental Data Analysis (CEDA) (University of East Anglia Climatic Research Unit ,2015).

3.5.11 Population

The WorldPop project (www.worldpop.org.uk), creates gridded data on the human populations within low and middle-income countries of the world. These data are derived from models that use information on settlements, land use and other geospatial data derived from satellite imagery, and

to disaggregate areal census population counts within 100x100m grid squares. Human population count was used for creating population-weighted averages for some of the indicators used in this study.

3.5.12 Urban/Rural

For this study the urban extents grid for the year 2000, produced by Columbia University Centre for International Earth Science Information Network (CIESIN) was obtained. The GRUMP urban areas dataset delineates urban locations in terms of population (5,000 or more inhabitants), settlement points and contiguous night-time lights (CIESIN - GRUMP (Global Rural Urban Mapping Project) (http://sedac.ciesin.columbia.edu/data/set/grump-v1-urban-extents). We also exploited the Global Human Settlements Layer (GHSL) (Pesaresi et al., 2013) representing built-up areas, quantified as the % of built-up coverage in a pixel. Percentage values are standardised to integer values between 0 and 255, such that 0 = 0% of built-up coverage and 255 = 100% of built-up coverage.

3.6 Modelling Architecture

Multiple approaches are available for creating predictive high-resolution spatial layers from a combination of geolocated household surveys and spatial covariate data. Here we exploit both machine learning and Bayesian geostatistical techniques (BGS) to construct the high resolution maps of stunting (Nigeria and Nepal) and wealth index (Nepal). The machine learning approach we used exploits Artificial Neural Networks (ANNs). This modelling architecture has at its basis the Geospatial Semantic Array Programming paradigm (GeoSemAP) (de Rigo et al., 2013; de Rigo, 2015; Bosco et al., 2017a; Bosco and Sander, 2015; Caudullo, 2014). To mitigate the modelling complexity and the inconsistencies between input data, parameters and output, semantic checks on the processed information and a modularisation of the key parts of the model were introduced following the Semantic Array Programming Paradigm (SemAP) as supported by the Mastrave modelling library (de Rigo, 2012a, 2012b, 2015). The proposed architecture also exploits the geospatial capacities of GIS systems. In our modelling approach we integrated SemAP and geospatial tools (ArcGis, GNU Octave and GNU R with GDAL) through GeoSemAP. GeoSemAP exploits geospatial tools and Semantic Array Programming for splitting a complex data-transformation-model (D-TM) into logical blocks whose reliability can more easily be checked by applying geospatial and mathematical constraints. Those constraints take the form of precondition, invariant and postcondition semantic checks. This way, even complex wide-scale transdisciplinary models may be described as the composition of simpler GeoSemAP blocks.

A handy formulation of models as data-transformation models (D-TM) is able to ease the integration of the various conceptual modelling-units (e.g. the machine learning and BGS modules) even when they are implemented in different programming languages. For example, two ANNs here exploited were implemented in two different programming languages (GNU R, GNU Octave). This is straightforward to achieve if these D-TM units exclusively exchange data (extended to include parameters, for example the parameters of an ANN after the training), with broadly supported formats. Data can be exchanged asynchronously also between D-TMs which physically run in different computational facilities (for example, the BGS module in GNU R run over a cloud cluster for the final map calculation, while the ANNs do not require such a demanding facility,

given their array-based approach where parts of the final map are computed asynchronously, e.g. exploiting the module mstream of the Mastrave modelling library).

In the effort toward increasing the reproducibility, as previously mentioned, free scientific software tools and libraries and freely available datasets were used in applying the geostatistical modelling techniques, and reproducible techniques were used for applying the models and submodels that are part of the modelling architecture.

3.6.1 Artificial Neural networks

An ANN is a data-transformation model, deriving a set of outputs starting from a set of input data. ANN use an architecture inspired by the human brain that acquires knowledge through a learning process and stores the acquired information within inter-neuron connection strengths (synaptic weights – which in their artificial implementation correspond to simple numerical parameters). Briefly, an ANN is built based on the concept of interconnected input data nodes, intermediary nodes and output nodes, with the number and type of nodes changing to suit the analyses. Nodes are connected to one another by weighted input functions. Once the network is built, the learning process takes place by iteratively adjusting the weighted connections between neurons then comparing the output to a desired calibration target. Because relationships between nodes need not be linear or even continuous, ANN architecture can more easily take advantage of complex relationships between covariate and output data. At the same time, data affected by large noise/signal ratios (or poor correlation with the desired quantity to model) may still be exploited by ANNs in their simplified near-linear relationships. Therefore, although the principal components (e.g. linear) of covariation might be easily discovered by ANNs even with factors showing a limited prediction power, the nonlinear components of relationship might also be exploited, when the unavoidable covariate-output noise allows these components to be numerically detected. A useful theoretical result applies to a particular family of ANNs (feed-forward multilayer perceptrons) which has the property of universal approximation, meaning that a properly designed and trained ANN in this family is virtually able to reproduce any relationship between input covariates and the quantity to be modelled (Hornik et al., 1989; Kreinovich, 1991).

Two feed-forward neural networks were applied in this study. The first ANN is a feed-forward multilayer perceptron (hence in the aforementioned family) implemented in MATLAB language in GNU Octave (Eaton, 2008). This modelling architecture was created exploiting the Neural network Package (Schmid, 2009) available in GNU Octave. The second ANN (also, a feed-forward multilayer perceptron) was implemented in GNU R (R Development Core team, 2014) using the structure available in the "AMORE" package (A MORE flexible neural network) (Castejón Limas et al., 2010). To conduct the model learning process, cross validation was applied (repeated random sub-sampling), wherein 70% of the data were used for training and 30% kept for validation of the final model. Parameters to be tuned included the number of neurons in each layer, the performance function (e.g. TAO (GNU R) or Mean-Square-Error (GNU Octave, GNU R)) and the activation function of the hidden and the output layers (Purelin, Tansig, Sigmoid, etc.). As a training algorithm, for GNU Octave the Levenberg-Marquardt approach was used, while other methods

were considered in the GNU R training, such as the adaptive gradient descendent, or the BATCH gradient descent.

3.6.2 Bayesian geostatistical models

As with standard linear modelling, geostatistical modelling approaches rely on exploiting the correlative relationships between covariate data and the measure of interest. The key difference is that, in a geostatistical framework, a model for the spatial autocorrelation between neighbouring datapoints is included (Banerjee et al., 2000). In the present context, a Bayesian modelling approach was used because of its flexibility to include hierarchical modelling structures and the ability to highlight areas where the model predictions have higher degrees of uncertainty. Here we opted to use the Integrated Nested Laplace Approximations (INLA) approach, available in the GNU R (R development core team, 2008) package called R-INLA (Rue et al., 2009). This approach provides a computationally-efficient approximation to a classic Markov-Chain Monte-Carlo approach. In addition, the R-INLA package includes the option to model output variables as a latent Gaussian Markov Random Field and to represent variation in the spatial dependence between data points using a Stochastic Partial Differential Equation approach (SPDE, Lindgren et al., 2011). This approach allows for continuous variation in the degree of spatial autocorrelation depending on the level of sampling available at each location and is well suited to producing high resolution maps for both the proportional stunting and wealth index variables.

Given the large number of covariates that were assembled for this project, to identify a limited number of them, suitable to prevent model overfitting and able to contribute to the highest possible explanatory power, a sensitivity analysis was conducted for each model. The covariate selection was based on a jackknife approach (Tukey, 1958) where, instead of selecting the best performing predictor at each stage of the methodology (with the risk of missing nonlinear patterns of correlation among multiple covariates), the worst performing was removed. Thus, the full set of covariates was assessed at each stage of the selection procedure, with an iterative removal of the ones less able to contribute to the overall model performance. The remaining subset was then used to train the models.

As with the ANN modelling, the selection of covariates was conducted via a repeated random sub-sampling cross-validation using 70% of the data in Nepal. Because of the larger dataset in Nigeria, data were split into training (60% of the data), test (20%) and validation (20%) subsets.

Each of these models required extensive calibration and testing. Because of this, after an initial test comparing the results of many different modelling architectures, we decided to apply only the more promising models in term of prediction capacity and computational effort. Bayesian models, when compared with ANNs, are considerably less time demanding but in general have similar predictive capacity (Bosco et al., 2017a, 2017b). Due to these characteristics, the majority of the maps we produced in Nepal on Wealth index are based on this family of models.

3.6.3 The Ensemble Approach

In modelling stunting in children under age of five in Nigeria we discovered a consistent discrepancy between modelling prediction capacity related to 2008 and 2013 datasets. In order

for the uncertainty to be mitigated, a robust ensemble approach was proposed to aggregate different maps of stunting related to the year 2008. Each of the discussed model architectures offers good performance under different conditions. In order to take advantage of the strengths of both modelling types and different training strategies of the two ANN implementations, we used a new ensemble approach to combine multiple model outputs, based on the stacked generalization (Wolpert, 1992). The stacking involves training a learning algorithm to combine the predictions of several other learning algorithms. In brief, the ensemble approach is a reproducible D-TM applied to the results of the array of models using a feed-forward artificial neural network based on the Levenberg-Marquardt algorithm as combiner. This approach is especially useful for data-poor regions for reducing locally-poor model performance as it allows the mitigation of outlier predictions. In order to further increase the ensembling training performance, a simplified version of the Selective Improvement Evolutionary Variance Extinction (SIEVE) (de Rigo et al., 2005) was applied to the ANN. The core of the SIEVE architecture is to use iteratively a selection of the best parameter vectors, reducing exponentially the number of parameter vectors surviving at the next iteration. This reduction of the parameter vectors is typically compensated for with an extension of the computational resources dedicated to train each parameter vector until the absolutely best vector passes the last SIEVE. The complete architecture of SIEVE includes also a "generative" phase within each step, where a cloud of new vectors are generated close to each parameter vector which survived the selection in the previous sieves. However, in this simplified application of SIEVE the performance were sufficiently improved even without introducing the generative steps.

3.7 Model Performance and Validation

To obtain the best performance in each of the countries and for each of the modelled variables, the prediction capacities of different models were compared. A two step Validation approach was applied in Nepal. In the first step, we applied a cross-validation on the training set of data (70% of the data) to select the best model in each of the tested modelling architectures. The relationship between predicted and observed values (the accuracy of the model) was quantified using the root mean square error (RMSE) and the mean absolute error (MAE). Although some authors suggest that inter-comparisons of average model-performance should be based on MAE (Willmott and Matsuura, 2005), we chose to also calculate RMSE due to its sensitivity to occasionally large predictive error. The remaining 30% of the data were used to measure modelling performance by calculating MAE, RMSE and the explained variance of the model (expressed in proportional terms). In Nigeria, due to the larger volume of data, we split the data into training, validation and testing sets (60-20-20).

Both in Nigeria and Nepal, the model with the highest value of explained variance and lowest RMSE and MAE was selected to be applied for producing the final map at 1x1 km resolution. For calculating the explained variance, we used the same equation applied in Bosco et al. (2015).

4. Results

Here we present the results of the predictive modelling exercises, first discussing the wealth index, then the results on modelling stunting. For each of the modelled indicators with an associated modelling explained variance higher than 0.5 in validation, we show maps of the survey clusters

and the indicator value at each cluster, maps of the predicted proportion of modelled indicators and the level of uncertainty associated with these maps in each pixel (figure 1, 2, 7, 8, and 14). We also present some analysis showing the changes of stunting in children and wealth index over time and how aid disbursement interacts with changes in these indexes (figure 3-6, 11, 12).

The poorest results were obtained when modelling stunting in Nepal (figure 13 and 14). Due to the lack of correlation between the available modelling covariates and this indicator, despite the effort done to collect new data (including travel to Nepal to gain access to new source of data), the modelling prediction performances were low (less than 30% explained variance in validation). These results are included in this report to show the work performed in the attempt to model this indicator and its relationship with aid disbursement, however the results are not compared against aid disbursement due to their lower quality.

4.1 Model performance characteristics

For all datasets and in both countries, BGS and ANNs had similar performance in terms of explained variance (Table 5). We were able to achieve explained variance over 50% for both stunting and wealth index in all time periods and both countries, except in the case of stunting in Nepal, where we were unable to surpass 30% of explained variance. These results are presented but not discussed further.

Table 5: Summary of model performance characteristics.

Country	Modelled Parameter	Modelling technique	MSE	RMSE	MAE	Exp.Var.	MSE (mean)
Nigeria	Stunting 2013	INLA	0.014	0.12	0.09	0.62	0.038
Nigeria	Stunting 2013	ANN(R)	0.016	0.129	0.10	0.62	0.038
Nigeria	Stunting 2008	ensemble	0.02	0.14	0.11	0.54	0.045
Nigeria	Stunting 2008	INLA	0.021	0.147	0.11	0.52	0.045
Nigeria	Stunting 2008	ANN(R)	0.023	0.153	0.12	0.48	0.045
Nigeria	Stunting 2008	ANN(Octave)	0.021	0.147	0.11	0.52	0.045
Nepal	Wealth Index 2006	INLA	0.3	0.54	0.4	0.72	1.04
Nepal	Wealth Index 2011	INLA	0.229	0.47	0.39	0.69	0.72
Nepal	Int. Wealth Index	INLA	162	12.7	10.2	0.60	407

	2006						
Nepal	Int. Wealth Index 2006	ANN (R)	165	12.8	10.3	0.60	407
Nepal	Int. Wealth Index 2011	INLA	150	12.2	9.7	0.59	359.5
Nepal	Stunting 2011	INLA	0.046	0.21	0.17	0.22	0.059
Nepal	Stunting 2011	ANN (R)	0.046	0.21	0.16	0.225	0.059

Wealth index

Wealth index in Nepal

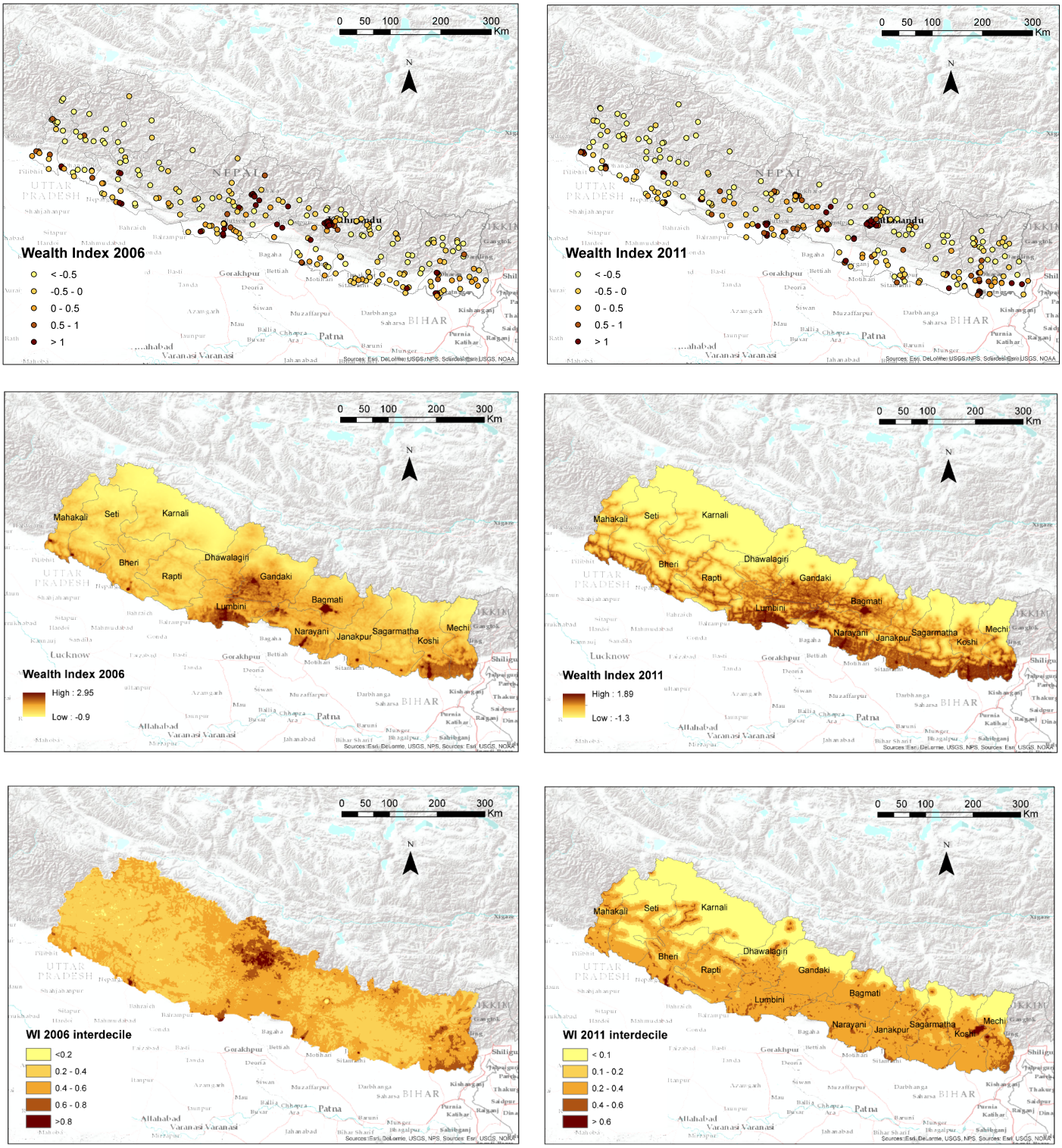

Figure 1: Map of the cluster-level survey data (top row), for the wealth index. Map of the wealth index in Nepal predicted at ~ 1 km spatial resolution (middle row) and associated uncertainty maps (interdecile) (bottom row).

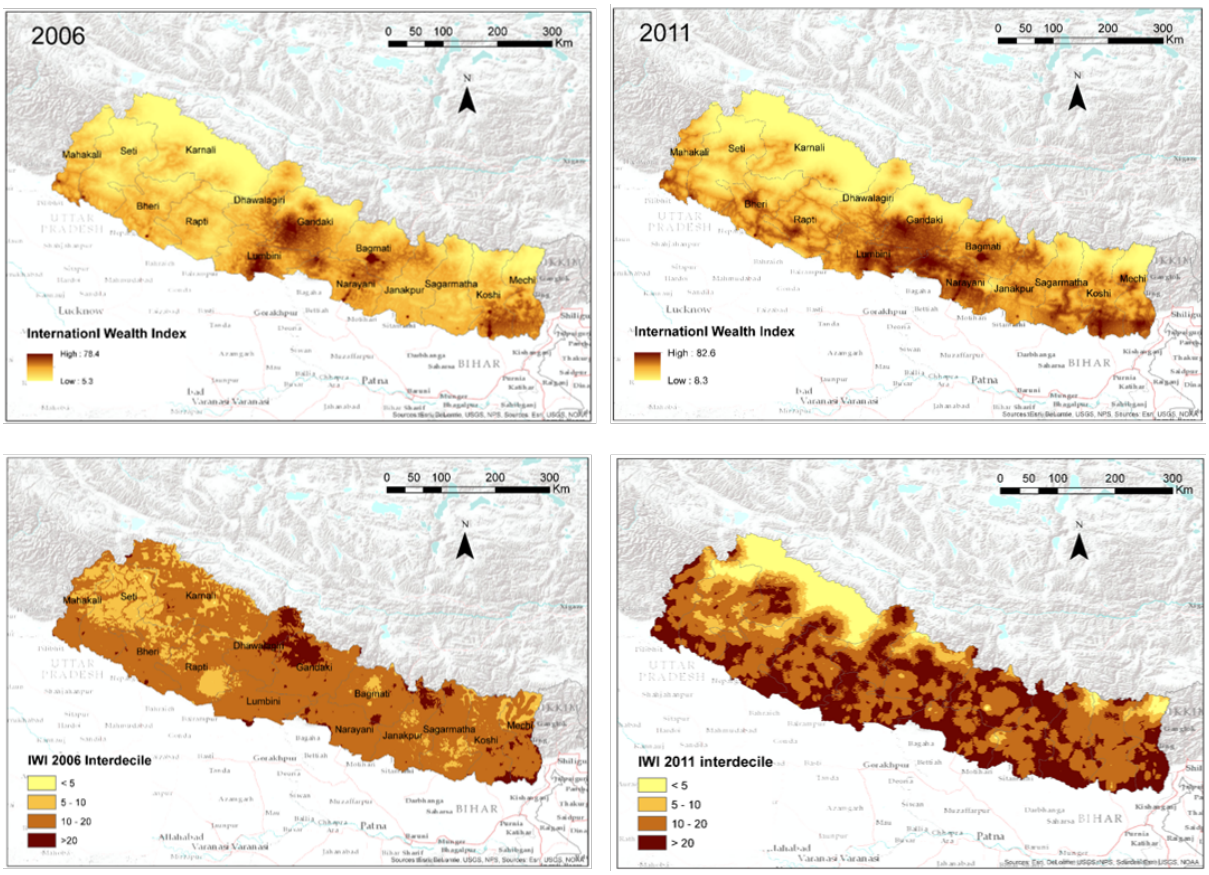

Figure 2: Map of international wealth index at ~ 1 km spatial resolution covering the whole Nepal (top row) and related uncertainty maps (interdecile) (bottom row).

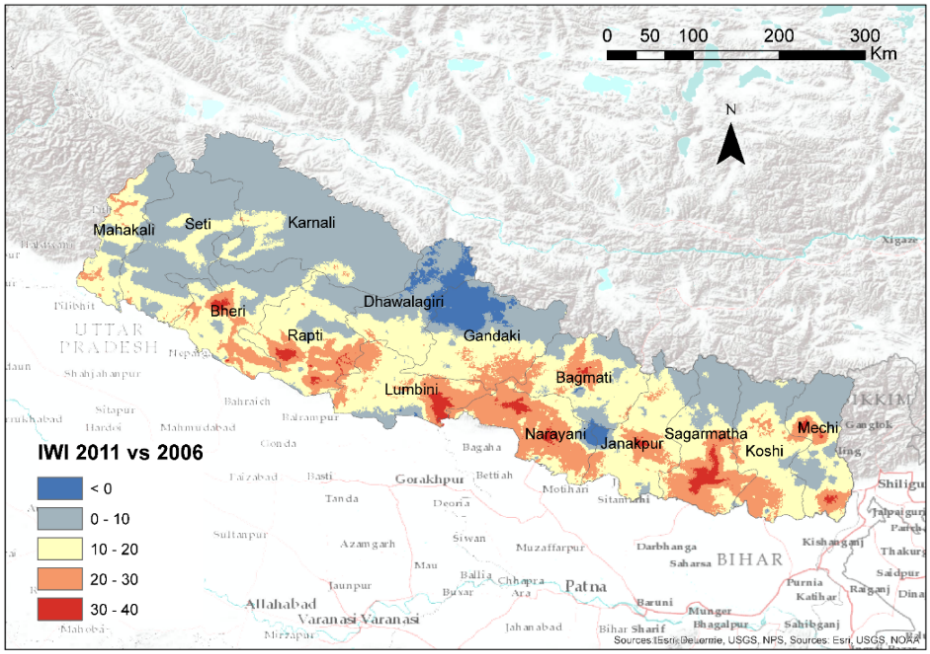

Figure 3: Change in international wealth index in Nepal for the years 2006 and 2011.

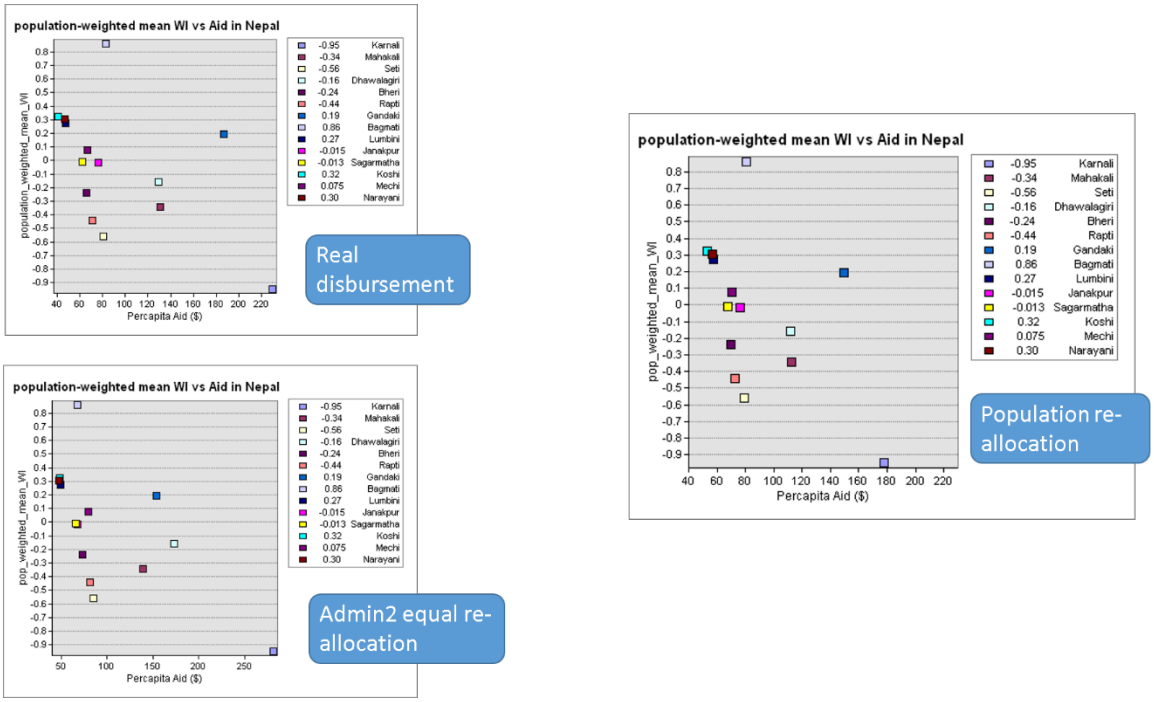

Figure 4: Population-weighted wealth index (2011) compared with different scenarios for how aid is disbursed in Nepal at ADMIN2 level (2001-2010). In the upper-left graph, Aid is re-allocated following real disbursement scenario, in the lower-left graph money are equally shared in each of the admin2 levels. In the graph on the right, money are re-allocated on the basis of the number of people living in each of these areas.

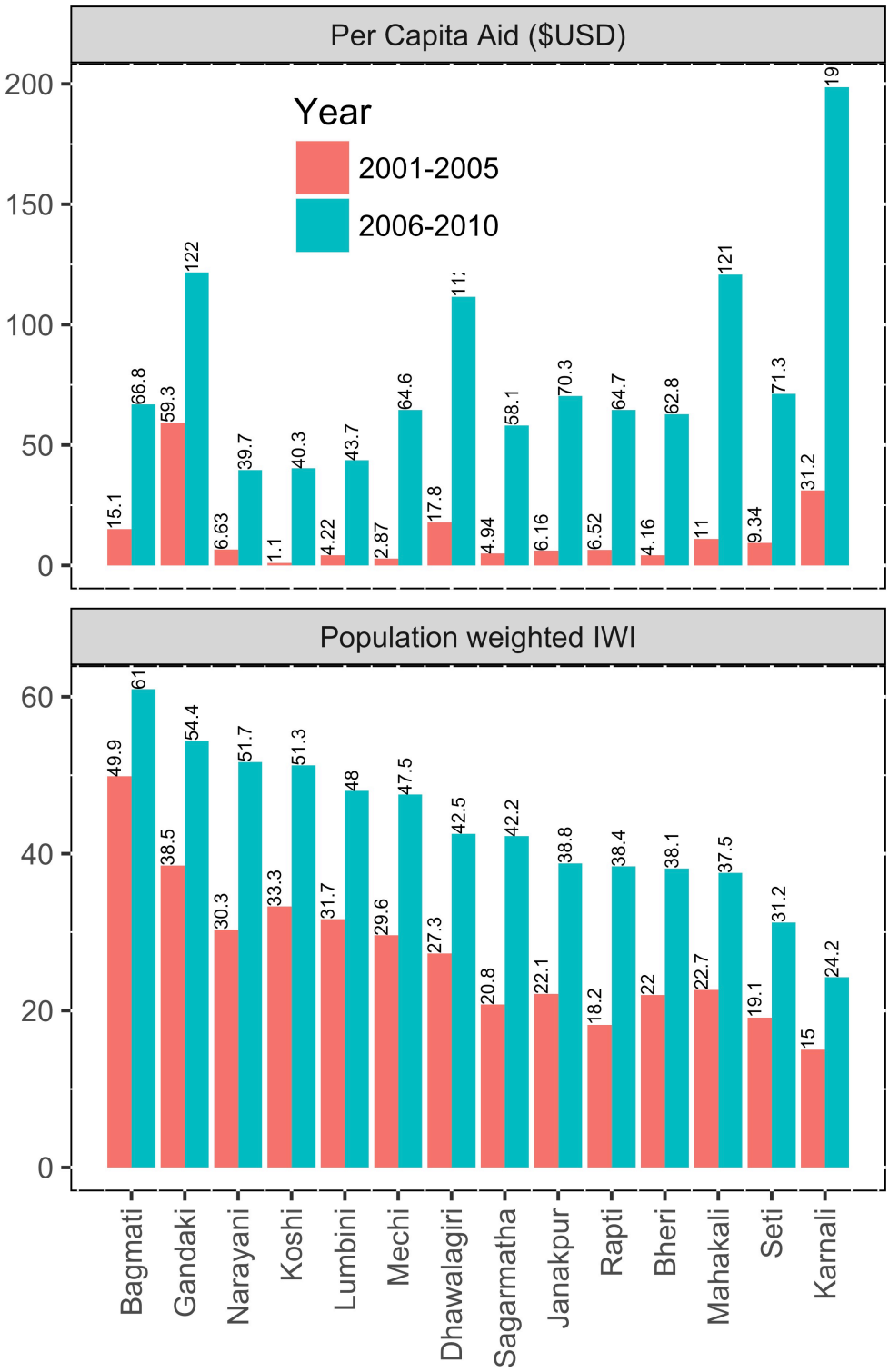

Figure 5: Top: Percapita Aid in Nepal related to the period 2001-2005 vs 2006-2010. Bottom: Comparison of the population weighted International Wealth Index at administrative 2 level for the year 2006 and 2011 in Nepal. Data were sorted following IWI values in 2006.

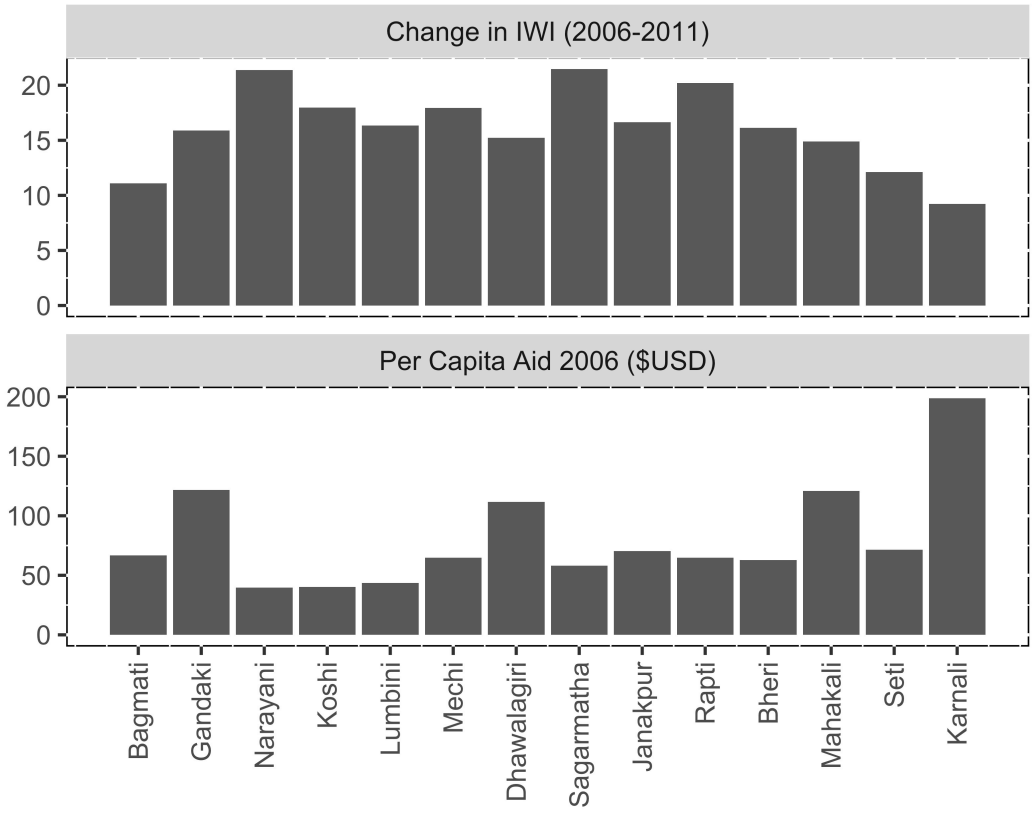

Figure 6: Top: Changes in the international wealth index from 2006 to 2010. Bottom: Per capita money spent in the same period for poverty alleviation in Nepal. The data follow the same sorting of admin 2 levels used in figure 5.

Stunting

Stunting in Nigeria

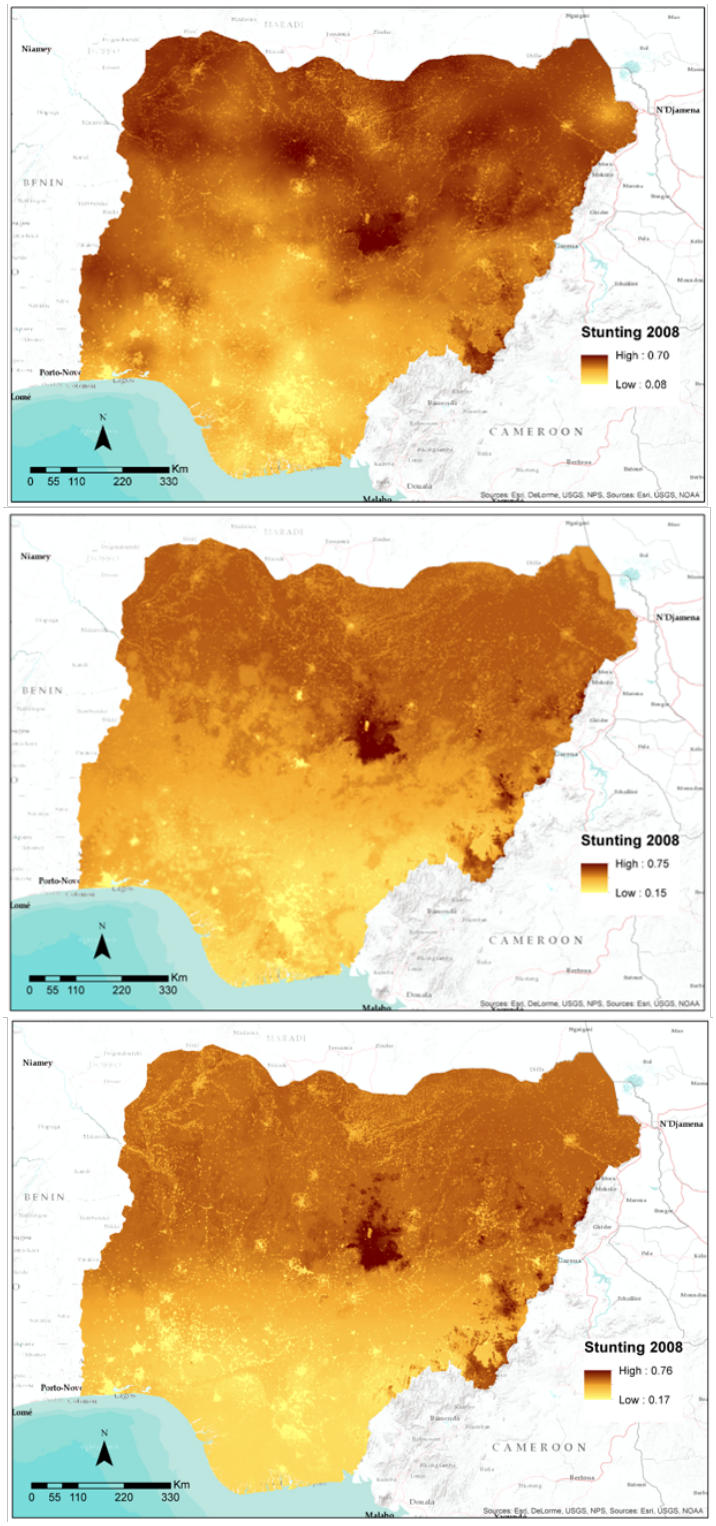

Figure 7: Maps of stunting in children in Nigeria related to the year 2008. These maps were created using a Bayesian geospatial model (INLA) (top row), and two feed-forward ANNs respectively implemented in GNU R (middle row) and GNU Octave (bottom row).

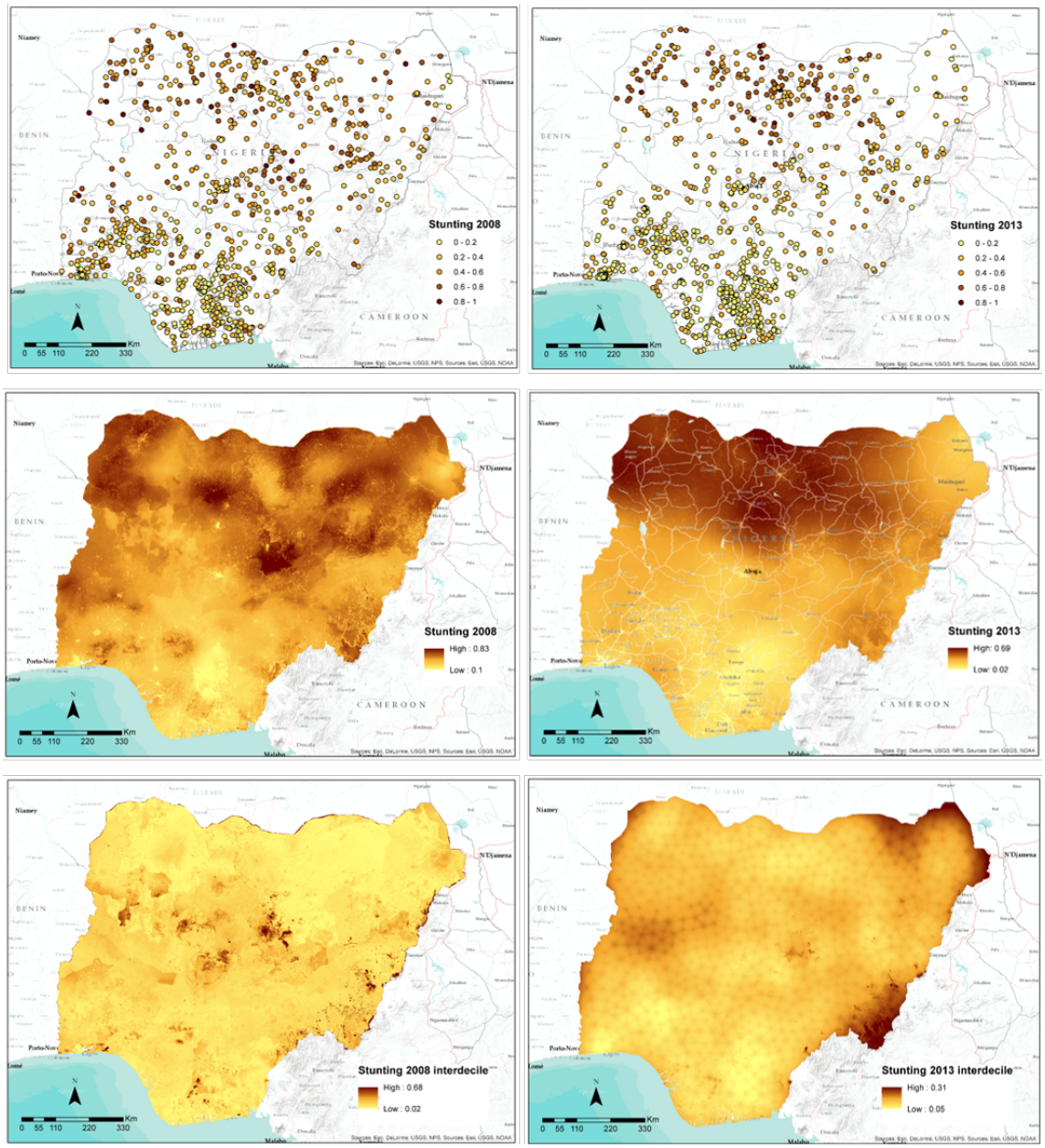

Figure 8: Map of the cluster-level survey data (top row), for stunting in children under age of five in Nigeria. Map of the stunting in Nigeria at 1 km spatial resolution (middle row) and associated uncertainty maps (interdecile) (bottom row). The map of stunting related to year 2008 was created by applying an ensemble approach on the output of an array of models (Fig. 7).

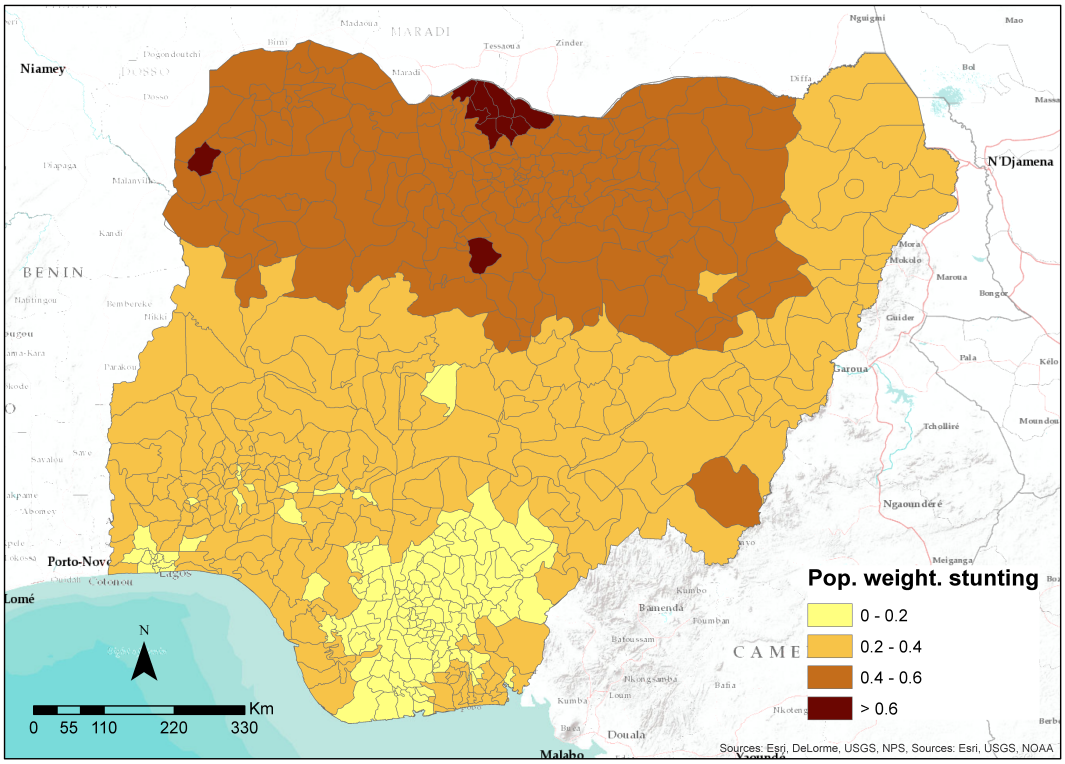

Figure 9: Map of stunting weighted by population related to the year 2013 at administrative 2 level

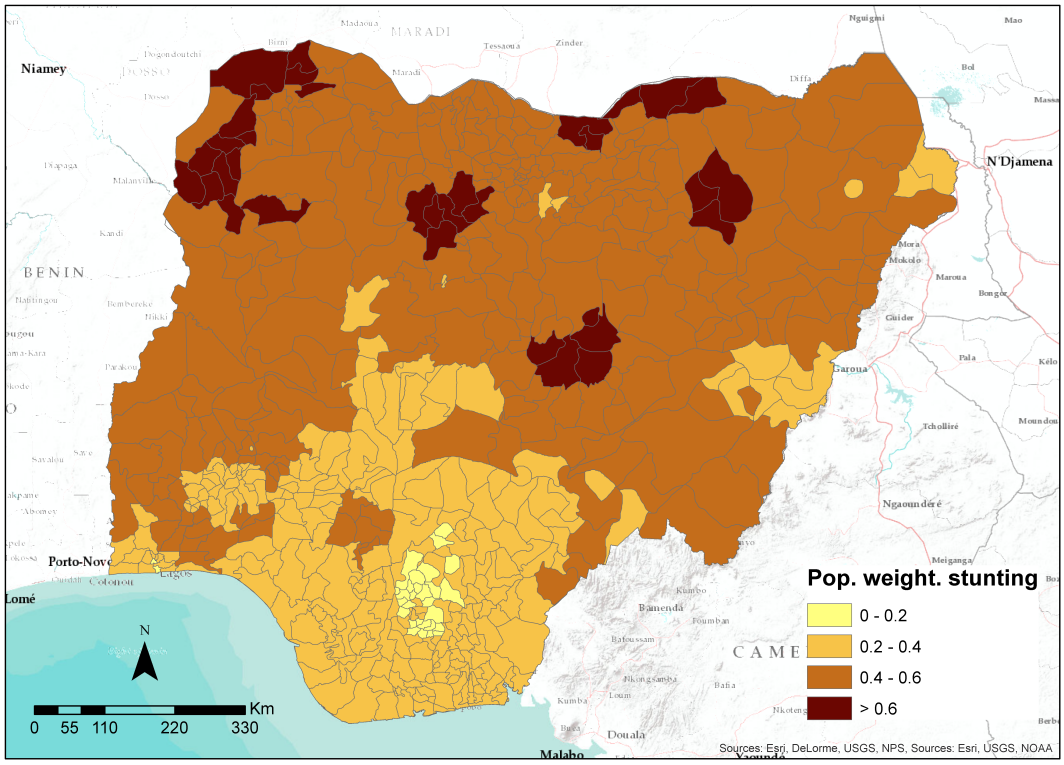

Figure 10: Map of stunting weighted by population related to year 2008 (administrative 2 level)

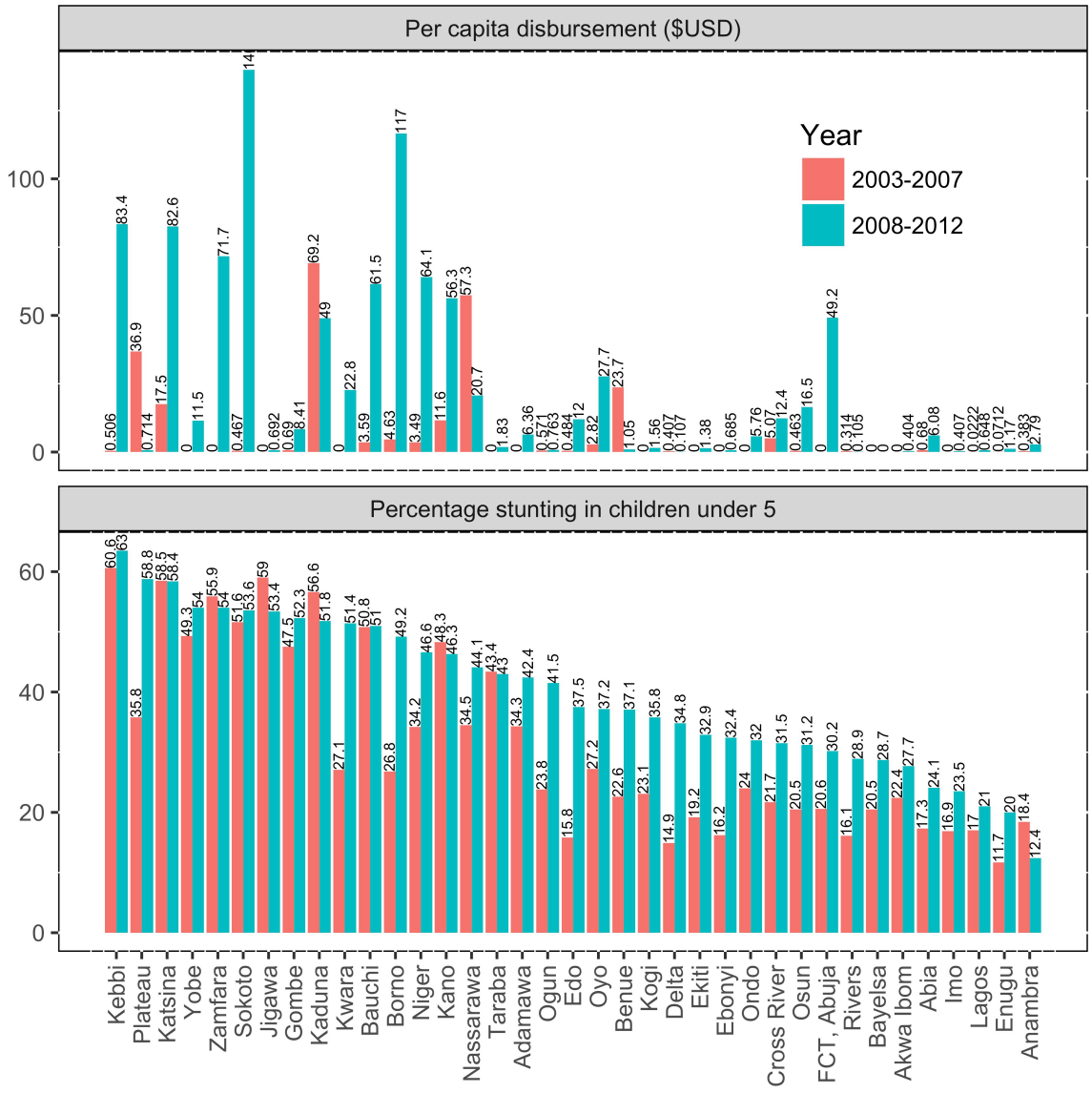

Figure 11: Top: Reported per capita disbursement for each state in Nigeria, ranked according to the percentage of stunted children under age of 5 (2008 values). Bottom: Proportion of the population weighted stunting in children under the age of 5 at administrative 1 level for the year 2008 and 2013 in Nigeria.

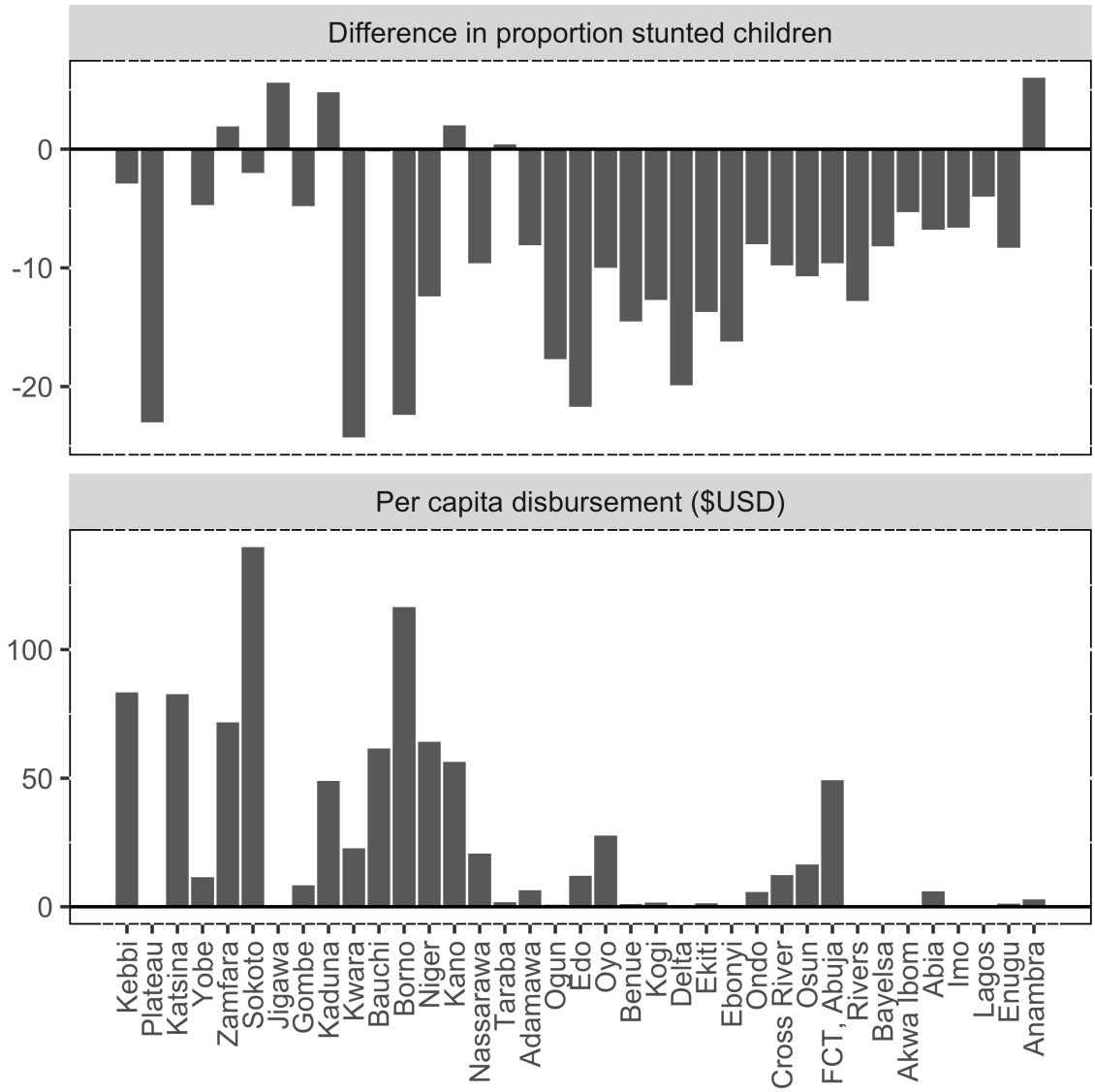

Figure 12: Graph illustrating the relationship between percapita money spent from 2008 to 2013 for stunting alleviation in Nigeria (Bottom) and the change in the stunting rate in the same period (Top). The same sorting of the administrative levels used in figure 11 was here applied.

Stunting in Nepal

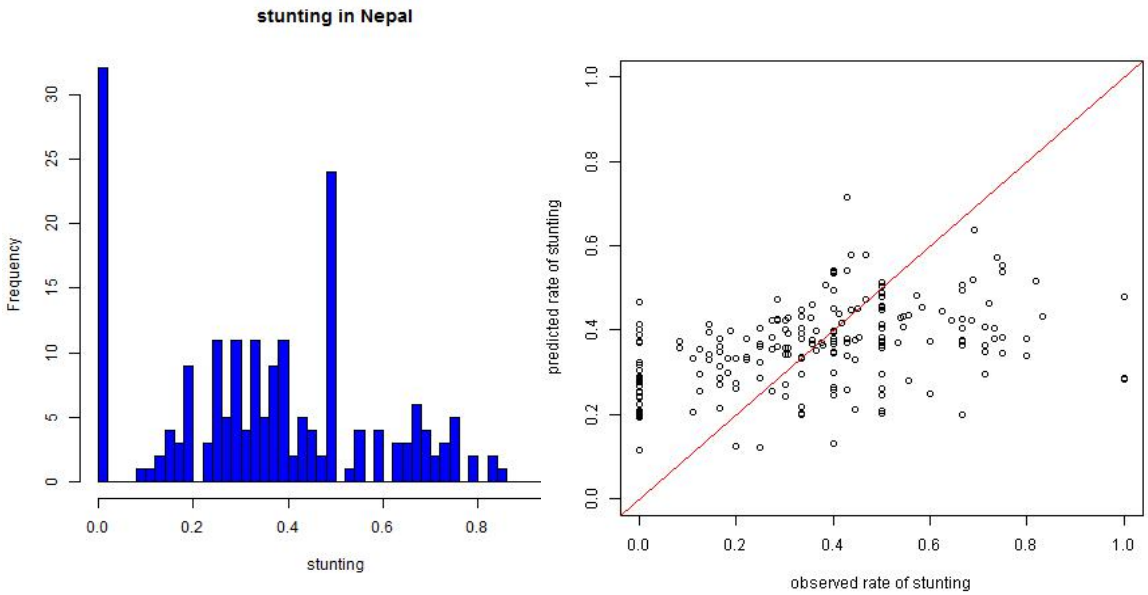

Figure 13: Histograms (left) showing the distribution of a 70% subset of DHS data (training) and scatter plot of the predicted (y-axis) and observed (x-axis) proportion of stunting in children under age of five in the training dataset.

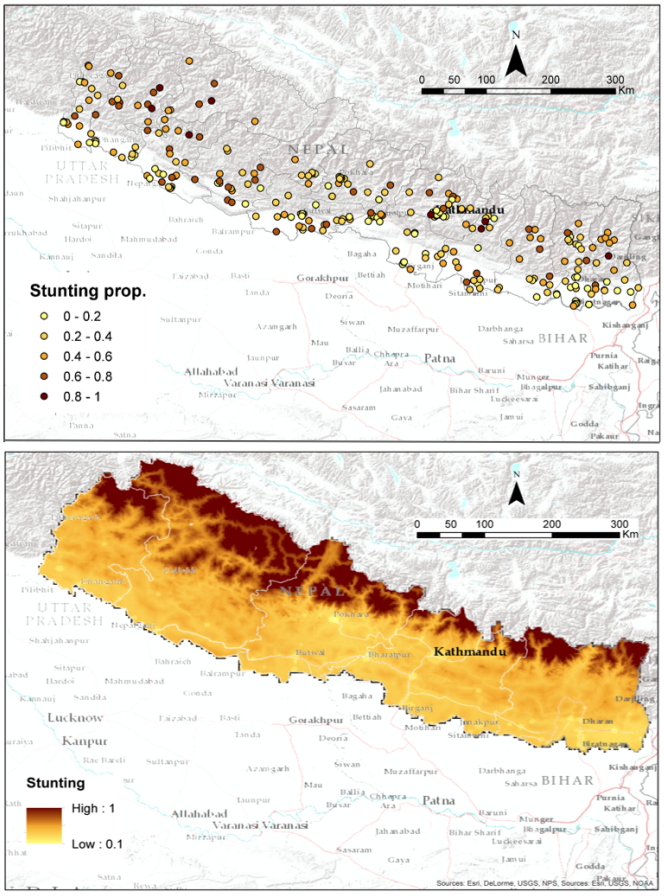

Figure 14: Map of cluster-level survey data (top row), for stunting in children under age of five in Nepal and map of the stunting at 1 km spatial resolution (bottom row).

5. Discussion

Results presented in this study show how detailed high resolution maps on different development indicators can be produced, starting from a combination of geolocated household surveys and spatial covariate data. The gridded outputs not only highlight heterogeneities that are masked at aggregate levels, but also provide a consistent format for integration with other datasets. This consistency lends itself well to comparisons with aggregated data sources such as DHS or MICS, which tend to be representative at higher regional levels.

However, the variety of approaches and models tested here highlights the challenge of obtaining reliable results in some contexts. The accuracy of each of these models, measured through the proportion of variance explained and the value of RMSE and MAE, varies depending on the country and indicator used, with some indicators performing very well in one country and not as well in others. For instance in the case of the wealth index in Nepal both in 2006 and 2011 models were able to explain around 70% of the variance in the data. By contrast, the model for stunting in Nepal (figure 13 and 14) showed lower accuracy levels. The reason for these differences in model performance are likely due to a combination of factors. First, a large component of the modeling success relates to the spatial heterogeneity in the indicator, as well as the degree of variability within a survey location. Where the level of heterogeneity is high at local levels, this can obscure any spatial trends. Further, the variables chosen for modeling may have little explanatory power when it comes to the indicator of interest. Previous work has linked a variety of geographic factors to indicators of population wellbeing such as poverty (Steele et al, 2017), stunting and literacy (Bosco et al, 2017a), child mortality (Pezzulo et al, 2017) and others. However in many cases the links between these factors and the indicators of interest may be weakly correlative. Thus, while significant effort was made to source and create potentially relevant covariates from readily available spatial data, it may often be the case that the variables chosen do not contain enough information to provide sufficient predictive power.

Within the present study, elevation, nightlights, percentage of urban areas, precipitation and the distance to roads emerged as important covariates for mapping indicators in various countries. For example the percentage of urban areas shows a correlation of respectively r=0.67 and r=0.4 with wealth index in Nigeria (referred to year 2011) and stunting in Nigeria (referred to year 2008). By contrast, stunting in Nepal had the highest correlation with elevation (r=0.3) and much lower correlations with other geospatial covariates.

Interestingly, we found that both the Bayesian geostatistical (BGS) techniques (INLA) and artificial neural networks (ANNs) were able to extract similar levels of predictive power from the available covariates (Table 5). In general it was expected that ANN would perform better due to their ability to detect and account for nonlinearities in the data sources and indeed ANN did tend to perform better. However the differences in performance were not as pronounced as expected. This result suggests that the BGS models did a good job of capturing the spatial autocorrelation in the data and using this information to predict into unsampled areas. The fact that BGS modelling resulted

in nearly the same level of explanatory power as ANN will mean that these approaches (which are available in relatively user-friendly R packages) and less prone to overfitting than ANNs, can be readily implemented in other scenarios. At the same time, the improvement of the ensemble approach over BGS and ANN shows that a combined approach can yield improved results which in some contexts may provide significant advantages.

Our most successful results were obtained when modelling wealth index in Nepal (Figure 1). Two maps at ~ 1 km spatial resolution were produced, derived by applying models able to respectively explain 0.69 (2011) and 0.72 (2006) of the variance. In its own right, this result presents a useful improvement to the resolution of data available and highlights the geographic variation in poverty within the country. Because the wealth index created by the DHS is not comparable between years, we produced two new maps using the International Wealth Index. While the explained variance present in maps for the IWI in 2011 and 2006 is slightly lower than for the wealth index (~60% for both) the results are suitable for the purpose of exploring the spatial distribution of aid relative to poverty.

A spatial analysis of the predicted wealth index in Nepal revealed the strong clustering and geographic pattern in this country, with population centres having higher wealth indices, and remote mountainous regions having much lower values (Figure 1). This pattern shows in the high resolution predictions as well, with gradients of WI radiating away from these. Similar patterns exist in both 2006 and 2011.

The uncertainty associated with both these maps is generally low. A North-South trends in the magnitude of uncertainty exist in the 2011 data, potentially reflecting greater variation in the South than the North. Maps of the International Wealth Index (IWI) showed similar patterns than the wealth index (Figure 2). Change in the IWI over time was also strongest in the southern regions, as well as clustered around urban centers (Figure 3).

One of the main challenges in leveraging the AidData database lies in the variable spatial precision of aid projects. Many projects only have information regarding the country to which aid was allocated, indicating a lack of information or allocation to a government department. Some scenarios to re-allocate money were tested (Figure 4), however in many cases it is impossible to test whether this reallocation of funds represents a plausible scenario. In each case we therefore had to make a best approximation.

Multiple comparisons of the disbursement of aid relative to need highlight both the inequality of aid distribution relative to need and the difficulty in obtaining a reliable quantification of each. For instance, comparisons of the disbursement of aid over time in Nepal shows that some regions obtain proportionally much higher levels of per-capita aid than others. The overall trend in aid allocation looks inverse to the trend in IWI (ranked in order of decreasing IWI for 2011), with standout anomalies in high aid allocation in the Gandaki, Bagmati (surrounding Kathmandu) and Dhawalagiri regions versus disproportionally low allocation in the Seti region (Figure 5). The

reason for these disparities is unclear. It is possible that some of the allocation to Bagmati and Gandaki regions are related to their proximity to the capital of Kathmandu, where many government and aid offices are located. Finally, some of these anomalies could be due to inaccurate reporting.

Comparing IWI maps between 2006 and 2011 a general positive trend towards poverty decreasing is evident (Figure 6). While it is impossible here to attribute causality between aid spending and this decrease in poverty over time, the observed changes are encouraging. Of particular note is the Karnali region, where the changes in poverty are lower than in other areas. This deviation from the overall trend is likely associated with the difficulty in accessing the region due to the poor road infrastructure and mountainous terrain. Thus, while per-capita spending on this region may be higher, the overall costs associated with delivery and logistics are said to be on the order of 7 x higher than other regions (Wagle, Nepal Planning Commission, Pers comm).

In Nigeria, two maps (2008 and 2013) were created (Figure 8). Modelling stunting in 2008 proved most challenging and the accuracy of this map was far from the results obtained in 2013. A possible explanation for this was a lack of covariates suitable to the earlier time period. For example, the percentage of urban areas is a significant predictor of population wellbeing in other contexts and one that has changed significantly over time in Nigeria. Thus, the correlation between urbanicity variables and stunting was likely weaker than they should have been. We anticipate that the paucity of urbanicity data will become less of a problem due to the increasing prevalence of satellite data globally, including offerings such as Facebook's recently released country-wide building delineations (Facebook Connectivity Lab, 2016) and updates to existing products such as the Global Urban Footprint (Esch *et al,* 2016).

In spite of this difficulty, we were able to implement a more robust modelling architecture based on the ensembling of three different models that were tested and applied in 2008 (Figure 7). The explained variance of the ensembled architecture is around 55%, not far from 62% obtained in 2013, again indicating how differing models can extract different information from the same sources.

By analysing the maps of predicted stunting in Nigeria, rural areas present an higher proportion of stunted children than urban areas (Figure 8) with population centres showing the lowest values. A north-south trend is evident by comparing 2008 and 2013 maps. The north-west of the country shows an increasing in the proportion of children stunted while the south goes towards a consistent stunting alleviation. The uncertainty associated with both these maps is generally low. Greatest uncertainty is present in those regions with sparse data.

Unfortunately when comparing aid disbursement with stunting in Nigeria, there was a significant lack of detailed geolocated information on aid disbursement (Table 2). As such, we were able to perform our analysis only at admin 1 level – the same level at which DHS data for the country are representative. The limited availability of data made a comparison of the aid spending between

periods challenging. We therefore ranked states in Nigeria according to the degree of stunting present in 2008 (figure 11). The corresponding pattern observed in 2013 shows a general improvement, with percentages of stunting in different administrative regions following a trend similar to the one in 2008. A similar trend was present in the disbursement in aid (2008-2012) relative to the proportion of stunting in the population, with regions receiving higher rates of per-capita funding generally having higher stunting in 2008. A few states stand out in terms of aid disbursements. Above average disbursement (relative to regions with similar stunting levels) was found in Sokoto and Borno states. The higher degree of expenditure in Borno is logical given the high degree of general poverty in this area, which is frequently subject to food shortages and intensive international aid work, as well as being subject to frequent violence from the Boko Haram militant group. The Sokoto region is also relatively impoverished, but no more so than other northern states such as Yobe, which we would also expect to receive substantial funding for development. Another stand-out state is the Federal Capital Territory of Abuja. Again, being a capital region it is likely that Abuja receives a substantial portion of support aimed at building logistic infrastructure, or as a hub from which aid is disbursed for minor projects.

In terms of places with lower funding than expected, the states of Yobe, Jigawa and Gombe are all located in areas of relatively high poverty. In the period 2007-2012, many other regions have zero (or close to zero) reported aid disbursements. Many southern states such as Lagos, Kogi, Ondo, Osun and Ebonyi are regions with relatively lower stunting and so lower per capita aid is expected. However the very low values reported here seem excessively so and we suspect either misreporting in many of these regions. In the period 2003-2007, the near-zero per-capita disbursement for most states is almost certainly false, probably linked with the lack of detailed spatial information for most of the projects.

In terms of change in stunting between 2008 and 2013, a strong difference was observed between these years with an overall trend towards stunting reduction despite some exceptions. .

6. Conclusion

The results presented in this study highlight that accurate high resolution maps of wealth index in Nepal (figure 1 and 2) and stunting in children under age of five in Nigeria (figure 7 and 8) can be produced. Because of their high predictive power these maps were summarized to policy- relevant administrative units to support decision makers for planning and resource allocation (figure 9 and 10). This work shows the value of exploiting advanced modelling architectures for combining geo-located household survey data with geospatial covariates layers. It allowed us to quantify not only the distribution of stunting and wealth index in low-income country but also to estimate the associated uncertainty. With household surveys regularly undertaken, monitoring of stunting and wealth index at country level is possible and potential exists for monitoring of these indicators at a larger scale.

This research presents results to help clarify where aid for stunting and poverty alleviation is needed most, how well this need has been covered by past funding and ultimately, whether the

giving of aid is related to observable changes in stunting rates. If in Nepal the picture coming from this study is clear enough to support policy maker in allocating future resource for poverty alleviation, in Nigeria the lack of adequate geographical information on aid disbursement hampered to create reliable statistics. From the perspective of funders, this level of end-to- end information will allow greater responsibility and responsiveness in the allocation of aid. At the most basic level, the use of maps in showing where aid is needed most will be a valuable tool for budgeting and allocation.

The ability to geolocate indices of need at high spatial resolution may provide a significant benefit transparency, efficiency and assessment, provided an equivalent understanding of the disbursement of aid are be recorded. However, while recording of spatial data on human population characteristics has a well-developed scientific pedigree, spatial record-keeping on aid allocation is arguably a much more difficult process due to political factors, logistic challenges and the diffuse nature of some spending relative to the populations being targeted. As a consequence, making the link between spending and need at higher spatial resolutions will require a more accurate and detailed tracking system and to model linkages accounting for spatial uncertainty.

References

AidData. 2016a. **Nigeria, Nigeria-AIMS_GeocodedResearchRelease_Level1_v1.3.1 geocoded dataset**. Williamsburg, VA and Washington, DC: AidData. (Last access: November 2017). http://aiddata.org/research-datasets

AidData. 2016b. Nepal, **Nepal-AIMS_GeocodedResearchRelease_Level1_v1.3.1 geocoded dataset**. Williamsburg, VA and Washington, DC: AidData. (Last access: November 2017). http://aiddata.org/research-datasets

Alegana, V.A., Atkinson, P.M., Pezzulo, C., Sorichetta, A., Weiss, D.,Bird, T., Erbach-Schoenberg, E., Tatem, A.J., 2015. **Fine resolution mapping of population age-structures for health and development applications**. *Journal of the Royal Society Interface 12*, 20150073+. https://doi.org/10.1098/rsif.2015.0073

Banerjee, S., Gelfand, A.E., Polasek, W., 2000. **Geostatistical modelling for spatial interaction data with application to postal service performance**. *Journal of statistical planning and inference 90*(1), 87-105. https://doi.org/10.1016/S0378-3758(00)00111-7

Blumenstock, J., Cadamuro, G., On, R., 2015. **Predicting poverty and wealth from mobile phone metadata**. *Science 350*(6264), 1073-1076. https://doi.org/10.1126/science.aac4420

Bosco, C., Alegana, V., Bird, T., Pezzulo, C., Hornby, G., Sorichetta, A., Steele, J., Ruktanonchai, C., Ruktanonchai, N., Wetter, E., Bengtsson, L., Tatem, A.J., 2017b. **Mapping indicators of female welfare at high spatial resolution**. Tech. rep., WorldPop project, Flowminder Foundation, Stockholm, Sweden. http://data2x.org/wp-content/uploads/2017/02/Mapping-Indicators-of-Female-Welfare-at-High-Spatial-Resolution.pdf , INRMM-MiD:14335578

Bosco, C., Alegana, V.A., Bird, T., Pezzulo, C., Bengtsson, L., Sorichetta, A., Steele, J., Hornby, G., Ruktanonchai, C.W., Ruktanonchai, N.W., Wetter, E., Tatem, A.J., 2017a. **Exploring the high-resolution mapping of gender-disaggregated development indicators**. *Journal of The Royal Society Interface 14*(129), 20160825+. https://doi.org/10.1098/rsif.2016.0825 , INRMM-MiD:14332252

Bosco, C., Sander, G., 2015. **Estimating the effects of water-induced shallow landslides on soil erosion**. *IEEE Earthzine 7*(2), 910137+. http://earthzine.org/?p=910137 , https://doi.org/10.1101/011965 , INRMM-MiD:13455081

Bosco, C., de Rigo, D., Dewitte, O., Poesen, J., Panagos, P., 2015. **Modelling soil erosion at European scale: towards harmonization and reproducibility**. *Natural Hazards and Earth System Science 15*(2), 225-245. https://doi.org/10.5194/nhess-15-225-2015 , INRMM-MiD:13508255

Burgert, C.R., Colston, J., Roy, T., Zachary, B., 2013. **Geographic displacement procedure and georeferenced data release policy for the demographic and health surveys**. DHS Spatial Analysis Reports, no. 7. Calverton, MD: ICF International.

Castejón Limas, M., Ordieres Meré, J.B., González Marcos, A., Martínez de Pisón Ascacibar, F.J., Pernía Espinoza, A.V., Alba Elías, F., 2014. **AMORE: A MORE Flexible Neural Network**

Package. R package version 0.2-12. https://cran.r-project.org/web/packages/AMORE/index.html

Caudullo, G., 2014. **Applying Geospatial Semantic Array Programming for a reproducible set of bioclimatic indices in Europe**. *IEEE Earthzine 7*(2), 877975+. http://www.earthzine.org/?p=877975 , https://doi.org/10.1101/009589 , INRMM-MiD:13385094

Christensen, Z., Nielsen, R., Nielson, D., Tierney, M., 2010. **Transparency Squared: The effects of donor transparency on recipient corruption levels**. In: Aid Transparency and Development Finance: Lessons and Insights from AidData, 22-25 March 2010. http://wp.peio.me/wp-content/uploads/2014/04/Conf4_Christensen-Nielsen-Nielsen-Tierney-01.10.2010.pdf

Cliff, A.D., Ord, J.K., 1975. **Model building and the analysis of spatial pattern in human geography**. *Journal of the Royal Statistical Society. Series B (Methodological) 37*(3), 297-348. http://www.jstor.org/stable/2984781

de Rigo, D., 2012a. **Semantic Array Programming with Mastrave - Introduction to semantic computational modelling**. The Mastrave project. http://mastrave.org/doc/MTV-1.012-1 , INRMM-MiD:11744308

de Rigo, D., 2012b. **Semantic Array Programming for environmental modelling: application of the Mastrave library**. In: Seppelt, R., Voinov, A.A., Lange, S., Bankamp, D. (Eds.), *International Environmental Modelling and Software Society (iEMSs) 2012 International Congress on Environmental Modelling and Software - Managing Resources of a Limited Planet: Pathways and Visions under Uncertainty, Sixth Biennial Meeting*. pp. 1167-1176. https://scholarsarchive.byu.edu/iemssconference/2012/Stream-B/69/ , INRMM-MiD:12227965

de Rigo, D., Corti, P., Caudullo, G., McInerney, D., Di Leo, M., San-Miguel-Ayanz, J., 2013. **Toward open science at the European scale: Geospatial Semantic Array Programming for integrated environmental modelling**. *Geophysical Research Abstracts 15*, 13245+. https://doi.org/10.6084/m9.figshare.155703 , INRMM-MiD:11977126

de Rigo, D., 2015. **Study of a collaborative repository of semantic metadata and models for regional environmental datasets' multivariate transformations**. Ph.D. thesis, Politecnico di Milano, Milano, Italy. http://hdl.handle.net/10589/101044 , INRMM-MiD:13769492

de Rigo, D., Castelletti, A., Rizzoli, A.E., Soncini-Sessa, R., Weber, E., 2005. **A selective improvement technique for fastening neuro-dynamic programming in water resources network management**. In: *Proceedings of the 16th IFAC World Congress (IFAC Praha 2005)*. http://folk.ntnu.no/skoge/prost/proceedings/ifac2005/Papers/Paper4269.html , http://hdl.handle.net/11311/255236 , INRMM-MiD:10793225

Drabek, Z., Payne, W., 2002. **The impact of transparency on foreign direct investment**. *Journal of Economic Integration 17*(4), 777-810. http://www.jstor.org/stable/23000835

Eaton, J.W., Bateman, D., Hauberg, S., 2008. **GNU Octave manual version 3: a high-level interactive language for numerical computations**. Network Theory Limited. ISBN: 0-9546120-6-X , http://www.network-theory.co.uk/docs/octave3/ , INRMM-MiD:9115371

Esch, T., Marconcini, M., Felbier, A., Roth, A., Heldens, W., Huber, M., et al., 2013. **Urban footprint processor - Fully automated processing chain generating settlement masks from global data of the TanDEM-X mission**. *IEEE Geoscienceand Remote Sensing Letters 10*(6), 1617-1621. https://doi.org/10.1109/LGRS.2013.2272953

European Space Agency (ESA), 2014. **Global Land Cover Map for 2000, 2005 and 2010**. (ESACCI-LC-L4 LCCS-Map-300m-P5Y-YEAR-v1.6.1.) http://catalogue.ceda.ac.uk/uuid/5dca9487dc614711a3a933e44a933ad3

Gething, P., Tatem, A., Bird, T., Burgert-Brucker, C.R., 2015. **Creating Spatial Interpolation Surfaces with DHS Data DHS Spatial Analysis**. Reports No. 11. Rockville, Maryland, USA: ICF International. https://dhsprogram.com/pubs/pdf/SAR11/SAR11.pdf

Gibson, J., Rozelle, S., 2003. **Poverty and access to roads in Papua New Guinea**. *Economic development and cultural change 52*(1), 159-185. https://doi.org/10.1086/380424

Golding, N., Burstein, R., Longbottom, J., Browne, A.J., Fullman, N., Osgood-Zimmerman, A., Earl, L., Bhatt, S., Cameron, E., Casey, D.C., Dwyer-Lindgren, L., Farag, T.H., Flaxman, A.D., Fraser, M.S., Gething, P.W., Gibson, H.S., Graetz, N., Kendall Krause, L., Rachel Kulikoff, X., Lim, S.S., Mappin, B., Morozoff, C., Reiner, R.C., Sligar, A., Smith, D.L., Wang, H., Weiss, D.J., Murray, C.J.L., Moyes, C.L., Hay, S.I., 2017. **Mapping under-5 and neonatal mortality in Africa, 2000–15: a baseline analysis for the Sustainable Development Goals**. *Lancet 390*(10108), 2171–2182. https://doi.org/10.1016/S0140-6736(17)31758-0

Grosh, M.E., Glewwe, P., 1995. **A guide to living standards measurement study surveys and their data sets**. Washington, DC: World Bank Publications.

Hornik, K., Stinchcombe, M., White, H., 1989. **Multilayer feedforward networks are universal approximators**. *Neural Networks 2*(5), 359-366. https://doi.org/10.1016/0893-6080(89)90020-8 , INRMM-MiD:1700245

ICF International, 2012. **Demographic and Health Survey Sampling and Household Listing Manual**. MEASURE DHS, Calverton, Maryland, U.S.A.: ICF International.

IUCN, UNEP-WCMC, 2015. **The World Database on Protected Areas (WDPA)** [Online], October 2015, Cambridge, UK: UNEP-WCMC. http://www.protectedplanet.net

Jarvis, A., Reuter, H.I., Nelson, A., Guevara, E., 2008. **Hole-filled SRTM for the globe Version 4**. Available from the CGIAR-CSI SRTM 90m Database. http://srtm.csi.cgiar.org

Jean, N., Burke, M., Xie, M., Davis, W.M., Lobell, D.B., Ermon, S., 2016. **Combining satellite imagery and machine learning to predict poverty**. *Science 353*(6301), 790-794. https://doi.org/10.1126/science.aaf7894

Kreinovich, V.Y., 1991. **Arbitrary nonlinearity is sufficient to represent all functions by neural networks: a theorem**. *Neural Networks 4* (3), 381-383. https://doi.org/10.1016/0893-6080(91)90074-f , INRMM-MiD:10833268

Land Processes Distributed Active Archive Center (LP DAAC), 2001. **MODIS/Terra Vegetation Indices (NDVI/EVI) 16-Day L3 Global 250m SIN Grid [Collection 5]**. NASA EOSDIS Land Processes DAAC, USGS Earth Resources Observation and Science (EROS) Center, Sioux Falls, South Dakota. (Last access: November 2017) https://lpdaac.usgs.gov

Lindgren, F., Rue, H., Lindström, J., 2011. **An explicit link between Gaussian fields and Gaussian Markov random fields: the stochastic partial differential equation approach**. *Journal of the Royal Statistical Society: Series B (Statistical Methodology) 73,* 423–498. https://doi.org/10.1111/j.1467-9868.2011.00777.x

Lloyd, C.T., Sorichetta, A., Tatem, A.J., 2017. **High resolution global gridded data for use in population studies**. *Scientific Data 4*, 170001+. https://doi.org/10.1038/sdata.2017.1

Macro International Inc., 1996. **Sampling manual. Demographic and health surveys phase III**. DHS III basic documentation, no.6. Calverton, MD: Macro International.

Ministry of Health and Population (MOHP) [Nepal], New ERA, and ICF International Inc., 2012. **Nepal Demographic and Health Survey 2011**. Kathmandu, Nepal: Ministry of Health and Population, New ERA, and ICF International, Calverton, Maryland.

Ministry of Health and Population (MOHP) [Nepal], New ERA, and Macro International Inc., 2007. **Nepal Demographic and Health Survey 2006**. Kathmandu, Nepal: Ministry of Health and Population, New ERA, and Macro International Inc.

Minot, N., Baulch, B., Epperecht, M., 2006. **Poverty and inequalityin Vietnam: spatial patterns and geographic determinants**. Research reports 148, International Food Policy Research Institute (IFPRI).

NOAA, 2014. **Version 4 DMSP-OLS Nighttime Lights Time Series (1992–201 3; Average Visible, Stable Lights, & Cloud Free Coverages)**. National Geophysical Data Center/US Air Force Weather Agency. Earth Observation Group. https://www.ngdc.noaa.gov/eog/dmsp/downloadV4composites.html

National Population Commission (NPC) [Nigeria] and ICF Macro, 2009. **Nigeria Demographic and Health Survey 2008**. Abuja, Nigeria: National Population Commission and ICF Macro.

National Population Commission (NPC), ICF International, 2014. **Nigeria demographic and health survey 2013**. Abuja, Nigeria and Rockville, pp. 566, MD: NPC and ICF International.

Nelson, A., 2008. **Estimated travel time to the nearest city of 50,000 or more people in year 2000**. Global Environment Monitoring Unit - Joint Research Centre of the European Commission, Ispra Italy. (Last access: November 2017). http://forobs.jrc.ec.europa.eu/products/gam/

Okwi, P.O., Ndeng'e, G., Kristjanson, P., Arunga, M., Notenbaert, A., Omolo, A., Henninger, N., Benson, T., Kariuki, P., Owuor, J., 2007. **Spatial determinants of poverty in rural Kenya**. *Proceedings of the National Academy of Sciences, 104*(43), 16769-16774. https://doi.org/10.1073/pnas.0611107104

Pesaresi, M., Huadong, G., Blaes, X., Ehrlich, D., Ferri, S., Gueguen, L., Halkia, M., Kauffmann, M., Kemper, T., Linlin Lu, Marin-Herrera, M.A., Ouzounis, G.K., Scavazzon, M., Soille, P., Syrris,

V., Zanchetta, L., 2013. **A global human settlement layer from optical HR/VHR RS data: concept and first results**. *IEEE Journal of Selected Topics in Applied Earth Observations and Remote Sensing 6*(5), 2102-2131. https://doi.org/10.1109/JSTARS.2013.2271445

Pezzulo, C., Bird, T., Utazi, E.C., Sorichetta, A., Tatem, A.J., Yourkavitch, J., Burgert-Brucker, C.R., 2016. **Geospatial Modeling of Child Mortality across 27 Countries in Sub-Saharan Africa**. DHS Spatial Analysis Reports No. 13. Rockville, Maryland, USA: ICF International.

R Development Core Team, 2014. **R: A language and environment for statistical computing**. R Foundation for Statistical Computing, Vienna, Austria.

Rue, H., Martino, S., Chopin, N., 2009. **Approximate Bayesian inference for latent Gaussian models using integrated nested Laplace approximations**. *Journal of the Royal Statistical Society: Series B (Statistical Methodology) 71*(2), 319-392. https://doi.org/10.1111/j.1467-9868.2008.00700.x

Rutstein, S., 1999. **Wealth versus expenditure: comparison between the DHS wealth index and household expenditures in four departments of Guatemala**. Calverton, Maryland: ORC Macro.

Rutstein, S.O., 2008. **The DHS wealth index: approaches for rural and urban areas**. Calverton, Maryland, USA: Macro International

Rutstein, S.O., Johnson, K., 2004. **The DHS wealth index**. DHS Comparative Reports No. 6. Calverton, Maryland, USA: ORC Macro.

Schmid, M.D., 2009. **A neural network package for Octave**. User's Guide Version: 0.1.9.1. http://www.plexso.com/61_octave/neuralNetworkPackageForOctaveUsersGu.pdf

Schulz S.F., 2009. **Disaster relief logistics: benefits of and impediments to cooperation between humanitarian organizations**. Haupt Verlag AG.

Sedda, L., Tatem, A.J., Morley, D.W., Atkinson, P.M., Wardrop, N.A., Pezzulo, C., Sorichetta, A., Kuleszo, J., Rogers, D.J., 2015**. Poverty, health and satellite-derived vegetation indices: their inter-spatial relationship in West Africa**. *International Health 7*(2), 99–106. https://doi.org/10.1093/inthealth/ihv005

Smits, J., Steendijk, R., 2015. **The international wealth index (IWI)**. *Social Indicators Research 122*(1), 65-85. https://doi.org/10.1007/s11205-014-0683-x

Steele, J.E., Sundsøy, P.R., Pezzulo, C., Alegana, V.A., Bird, T.J., Blumenstock, J., et al., 2017. **Mapping poverty using mobile phone and satellite data**. *Journal of The Royal Society Interface 14*(127), 20160690+. https://doi.org/10.1098/rsif.2016.0690

Tatem, A.J., 2014. **Mapping the denominator: spatial demography in the measurement of progress**. *International Health 6*(3), 153-155. https://doi.org/10.1093/inthealth/ihu057

Tatem, A.J., Campbell, J., Guerra-Arias, M., de Bernis, L., Moran, A., Matthews, Z., 2014. **Mapping for maternal and newborn health: the distributions of women of childbearing age, pregnancies and births**. *International Journal of Health Geographics 13*, 2+. https://doi.org/10.1186/1476-072X-13-2

Tukey, J.W., 1958. **Bias and confidence in not-quite large samples**. Annals of Mathematical Statistics, 29, 614.

UNDP, 2016. **Human development report 2016: human development for everyone**. 286 pp. Washington, DC: UNDP. ISSN: 0969-4501

US NOAA National Geophysical Data Center/US Air Force Weather Agency, 2014. **Version 4 DMSP-OLS Nighttime Lights Time Series (1992-2013; Average Visible, Stable Lights, & Cloud Free Coverages)**. Earth Observation Group http://ngdc.noaa.gov/eog/dmsp/downloadV4composites.html

United Nations, 2016. **The sustainable development goals report 2016**. New York, NY: United Nations Publications, pp. 56.

University of East Anglia Climatic Research Unit; Harris, I.C.; Jones, P.D., 2015**. CRU TS3.23: Climatic Research Unit (CRU) Time-Series (TS) Version 3.23 of High Resolution Gridded Data of Month-by-month Variation in Climate (Jan. 1901 - Dec. 2014)**. Centre for Environmental Data Analysis, 09 November 2015. https://doi.org/10.5285/4c7fdfa6-f176-4c58-acee-683d5e9d2ed5

Willmott, C.J., Matsuura, K., 2005. **Advantages of the mean absolute error (MAE) over the root mean square error (RMSE) in assessing average model performance**. *Climate research 30*(1), 79-82. http://www.jstor.org/stable/24869236

Wolpert, D., 1992. **Stacked generalization**. Neural Networks 5(2), 241-259. https://doi.org/10.1016/S0893-6080(05)80023-1 , INRMM-MiD:3157859

World Bank, 2016. **LSMS - living standards measurement study**. http://surveys.worldbank.org/lsms